Whereas those observations suggest the positive role of PKDs in immune responses, it was shown that PKD2 was responsible for the interferon α-induced phosphorylation of a degron of the α interferon receptor and therefore for its accelerated degradation by ubiquitination, which could neutralize the defensive functions of type I IFN [18].

In the present work, we identified one of the phosphorylation sites of SET protein by PKD2 and potential role of SET phosphorylation by PKD2 is discussed.

Methods

Cells and reagents

Human leukemic T cell line Jurkat (E6-1) was obtained from American Type Culture Collection (Manassas, VA). Jurkat cells expressing GFP-tagged constitutively active (CA) mutant and GFP-tagged kinase dead (KD) mutant of PKD2 (CA-PKD2-GFP and KD-PKD2-GFP, respectively) were prepared as reported previously [12]. Jurkat cells expressing GFP-tagged wild-type SET (GFP-SET-WT) and SET S171A mutant (GFP-SET-S171A) were prepared by introducing pAcGFP1-C1 vector (Clontech, Mauntain View, CA) inserted with SETβ cDNA and the mutant SETβ cDNA, respectively. Anti-human CD3ε mAb (UCHT-1) and anti-GFP antibody were purchased from BD Biosciences (Franklin Lakes, NJ). Anti-human PKD2 antibody and anti-human SET antibody were from Bethyl Laboratories (Montgomery, TX). Anti-PP2A C-subunit phospho-Tyr307 antibody, anti-phospho-P44/42 MAPK (Thr202/Tyr204) and anti-ERK1 (K-23) sc-94 antibodies were from Epitomics (Burlingame, CA), Cell signaling (Danvers, MA) and Santa Cruz Biotechnology (Santa Cruz, CA), respectively. Anti-mouse IgG $F(ab')_2$ fragment was from PIERCE Biotechnology (Rockford, IL). Myelin basic protein (MBP, dephosphorylated), anti-PP2A C-subunit antibody and purified PP2A AC heterodimer were obtained from Upstate Biotechnology (Lake Placid, NY). Gö6976 and Gö6983 were from Calbiochem (San Diego, CA). Jurkat cell nuclear extract was purchased from Active Motif (Carlsbad CA). Poly-L-Lysine Agarose and phytohemagglutinin (PHA) were form Sigma-Aldrich (St. Louis, MO).

Plasmid

Full-length human SETβ cDNA was obtained from total RNA of Jurkat cell using RT-PCR and inserted into a pET28a vector (Novagen, Darmstadt, Germany) for preparation of recombinant proteins or a pAcGFP1-C1 vector for Jurkat cell-transfection. Mutations of SET were introduced by overlapping PCR.

Cell stimulation

Jurkat cells were stimulated with anti-CD3ε mAb (2 μg/ml) for 10 min followed by addition of anti-mouse IgG $F(ab')_2$ fragment (8 μg/ml) and stimulated for 1 h at 37°C, or stimulated with PHA (2 μg/ml) at 37°C for 12 hrs. Human $CD4^+$ T cell clone was stimulated by co-culturing with mouse L cells expressing its cognate ligand [19] HLA-DR4 (DRB1*04:06) covalently linked with streptococcal M12p54-68 peptide for indicated periods as described previously [9,12,20,21].

Quantitaion of phosphorylated SET

Jurkat cells expressing GFP-SET-WT were stimulated by PHA and lysed using a lysis buffer supplied with a PhosphoProtein Purification Kit (Qiagen) according to the manufacturer's instruction. In some experiments, cells were treated under the presence of PKD2 inhibitor Gö6976 (3 μM) before and during the PHA stimulation or the cells were treated with siRNA as described below before the stimulation. The fluorescence of GFP in the lysate was measured at excitation 475 nm and emission 505 nm using a Hitachi Fluorescence Spectrometer F-2500 (Tokyo, Japan). Each lysate containing the same amount of fluorescence was applied to the PhosphoProtein Purification Columns (Qiagen). Phospho-GFP-SET-WT recovered was subjected to SDS-PAGE and transferred onto a PVDF membrane. The phospho-GFP-SET-WT was detected and quantified by anti-GFP antibody and horseradish peroxidase-conjugated secondary antibody followed by enhanced chemiluminescent detection (ECL, Amersham Biosciences).

2D-gel electrophoresis and mass-spectrometric analysis

Jurkat cells (1×10^7) treated with anti-CD3ε mAb and anti-mouse IgG $F(ab')_2$ fragment were lysed and immunoprecipitated with anti-PKD2 antibody as described previously [12]. After washing, the beads were incubated in the kinase buffer (30 mM Tris-HCl, pH 7.4, 10 mM $MgCl_2$ and 1 mM DTT) containing 16 μg of heat-inactivated (50°C, 5 min) Jurkat nuclear extract (Active Motif) and either 0.25 MBq [γ-^{32}P]-ATP or 25 μM cold ATP at 30°C for 10 min. The kinase reaction with [γ-^{32}P]-ATP was performed in the presence of 3 μM of Gö6983 or Gö6976. Both kinase reaction mixtures with hot and cold ATPs were submitted to isoelectric focusing on pH 3–10 non-linear immobilized pH gradient strips (7 cm, Bio-Rad) followed by 11% second dimension SDS- PAGE in parallel. After the gels were stained with syproruby reagent (Bio-Rad), the gels with radioactivity were sandwiched with clear cellophane sheets, dried and exposed to X-ray films (Fujifilm, Tokyo, Japan). UV-illuminated dried gel sheets were overlaid onto the developed X-ray films to identify radioactive protein spots. The corresponding syproruby-stained protein spots on the cold gels were excised and subjected to trypsin-digestion and mass-spectrometric analysis.

Expression and purification of recombinant SET proteins

pET28a-SET plasmids were introduced into BL21(DE3) *E. coli* strain (Novagen). The 6×His-tagged SET protein expression was induced according to the manufacturer's instruction. The bacterial pellet was sonicated and the soluble recombinant SET proteins were fractionated by poly-L-lysine-agarose beads column according to the method described by Li *et al.* [2]. Fractions with recombinant SET proteins were combined, dialyzed and applied to a Ni-NTA resin column (0.5 ml, Qiagen). The SET protein was eluted with a 20 mM Tris-HCl (pH 8.0) buffer containing 500 mM NaCl and 500 mM imidazole. The fractions were combined and dialyzed against 50 mM Tris-HCl, pH 7.0.

In vitro PP2A phosphatase assay

Dephosphorylated MBP was ^{32}P-labeled by recombinant PKA (New England BioLabs) according to the manufacturer's instruction. ^{32}P-MBP, recombinant SET proteins and purified PP2A (Upstate) were diluted with phosphatase buffer (50 mM Tris-HCl, pH 7.0, 50 μg/ml BSA, 1 mM DTT, 0.25 mM $MnCl_2$). After mixing 16 μl of indicated concentrations of the recombinant SET and 2 μl PP2A (37 μU) and incubating at 4°C for 15 min, 2 μl ^{32}P-MBP was added and left at 37°C for 10 min. The reaction was stopped by adding 6 μl of sample buffer and 20 μl of the reaction mixture was subjected to 15% SDS-PAGE. The gels were dried and the remaining radioactivity of MBP was quantified by BAS-2000 image analyzer (Fujifilm). In *ex vivo* experiments, the PP2A phosphatase activity from Jurkat or human $CD4^+$ T cell clone were estimated by the phosphorylation status at Tyr307 of the catalytic subunit of PP2A by western blotting using anti-PP2A C-subunit phospho-Tyr307 [22].

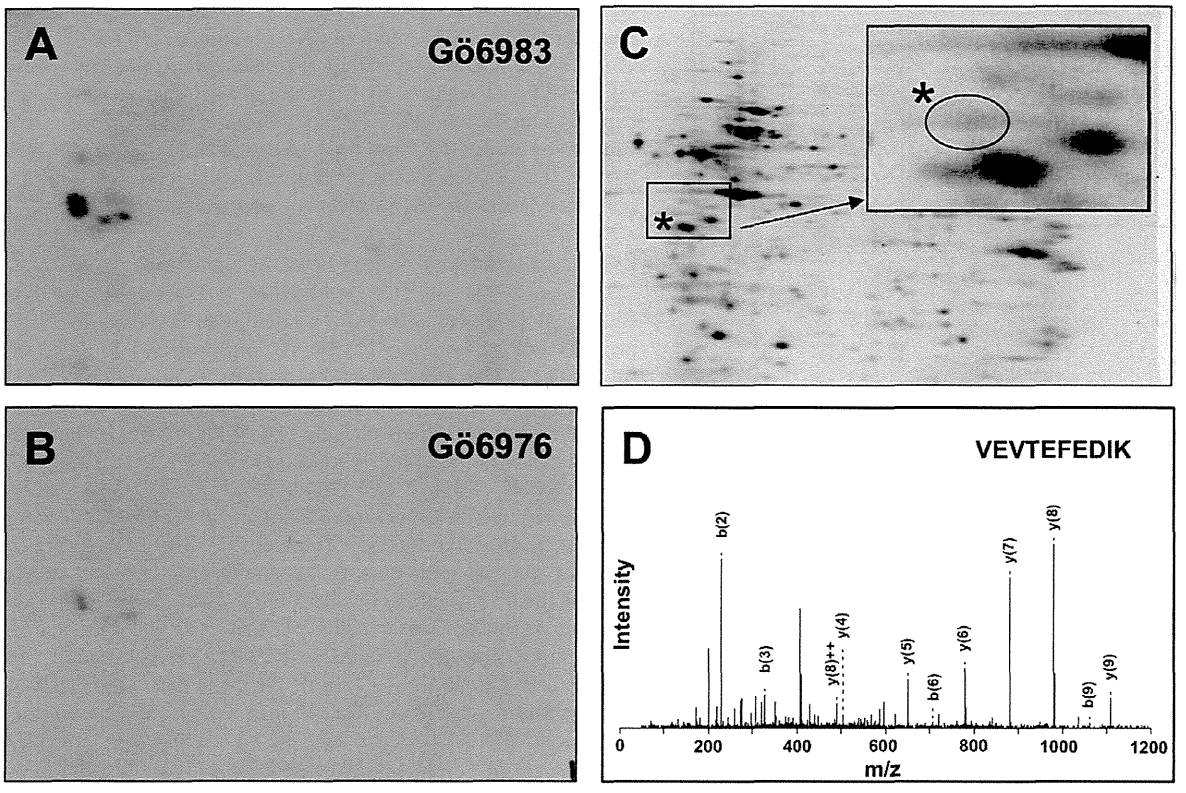

Figure 1. SET protein in Jurkat nuclear extract is phosphorylated by PKD2. Activated PKD2 was immunoprecipitated from lysate of Jurkat cells stimulated with anti-CD3ε antibody. The heat-inactivated (50°C, 5 min) Jurkat nuclear extract was used as a substrate for PKD2 and analyzed by 2D-gel electrophoresis. (A) Activated PKD2 was incubated with the nuclear extracts in the presence of [γ-^{32}P]-ATP and Gö6983 (an irrelevant PKC inhibitor) and the radioactivity of 2D-electrophregram was detected. (B) Activated PKD2 was incubated with the nuclear extracts in the presence of [γ-^{32}P]-ATP and Gö6976 (PKD2 inhibitor) and the radioactivity of 2D-electrophoregram was detected. (C) The proteins in the Jurkat nuclear extract treated with non-radioactive ATP and PKD2 were stained with syproruby. Inset; the enlarged view of the boxed area. A protein spot indicated by the asterisks, which overlaps to the radioactive spots indicated in A or in B was analyzed by mass spectrometry. (D) One of the MS/MS spectra assigned to be SET protein is shown (m/z = 604, ^{110}VEVTEFEDIK^{119}).
doi:10.1371/journal.pone.0051242.g001

Knockdown of PKD2 by RNA interference

siRNAs for human *PKD2* were designed as follows: siRNA1 sense, 5′-GACAAACUGCGCUUCCCUACC-3′ and antisense, 5′-UAGGGAAGCGCAGUUUGUCAA-3′; siRNA2 sense, 5′-GUUCGAGACGCCUGAGAAAGU-3′ and antisense, 5′- UUU-CUCAGGCGUCUCGAACAU-3′. Three μl of each duplex siRNA (100 μM) was added to Jurkat cell suspension (1.5×10^7/100 μl) and electroporated with a Nucleofector II (Lonza) according to the manufacturer's instructions. The siRNA1 had no effect on PKD2 expression level and used as a negative control.

Western blotting

Jurkat cells (1.5×10^6) or human CD4$^+$ T cell clone (1.5×10^6) were lyzed with 15 μl of the lysis buffer (1% NP-40, 0.1% SDS, 0.5% sodium deoxycholate, 10% glycerol, 20 mM Tris/HCl-pH 7.4, 150 mM NaCl, 1 mM Na_3VO_4, 10 mM NaF, 1 mM EDTA, 1 mM EGTA, and a protease inhibitor cocktail tablet from Roche) and the supernatant was subjected to SDS-PAGE. The proteins were electro-blotted onto a PVDF membrane. PKD2, SET, GFP-tagged recombinant SET proteins, ERK1, phospho-ERK and β-actin were probed with respective antibodies and horseradish peroxidase-conjugated secondary antibody followed by the ECL detection. A lumino image analyzer (LAS-4000, Fujifilm) was used to quantify the chemiluminescence.

Results

SET protein is a candidate substrate for PKD2

Since activated PKD2 translocates into the nucleus [12], we performed *in vitro* kinase assay using Jurkat cell nuclear extract to screen potential PKD2 substrates. The Jurkat cell nuclear extracts were equally divided into three tubes and each was subjected to the kinase reaction. Two of them were subjected to the kinase reaction with ^{32}P-ATP and a pan-PKC inhibitor Gö6983 (Fig. 1A) that does not inhibit PKD kinase activity [23], or a PKD2 inhibitor Gö6976 (Fig. 1B). The third tube was subjected to the reaction with cold ATP without inhibitors (Fig. 1C). Incorporation of radioactivity was not observed in the gel when the nuclear extracts were treated with ^{32}P-ATP without adding PKD2 (data not shown), showing the back ground kinase activity in the nuclear extract was well inactivated by mild heat inactivation. As shown in Fig. 1A, some radioactive spots were observed in the 2D-gel that were phosphorylated in the presence of Gö6983, but markedly suppressed in the presence of Gö6976 (Fig. 1B), indicating that the proteins were specifically phosphorylated by PKD2. The gels were stained with syproruby and the protein spots corresponding to the radioactivity were excised from the non-radioactive gel (Fig. 1C). The gel pieces were subjected to in-gel trypsin digestion and the tryptic fragments were analyzed by an ESI-Q-TOF mass-spectrometer (Qstar Pulser *i*, Applied Biosystems, Foster City, CA). The MS/MS analysis (Fig. 1D) suggested the presence of

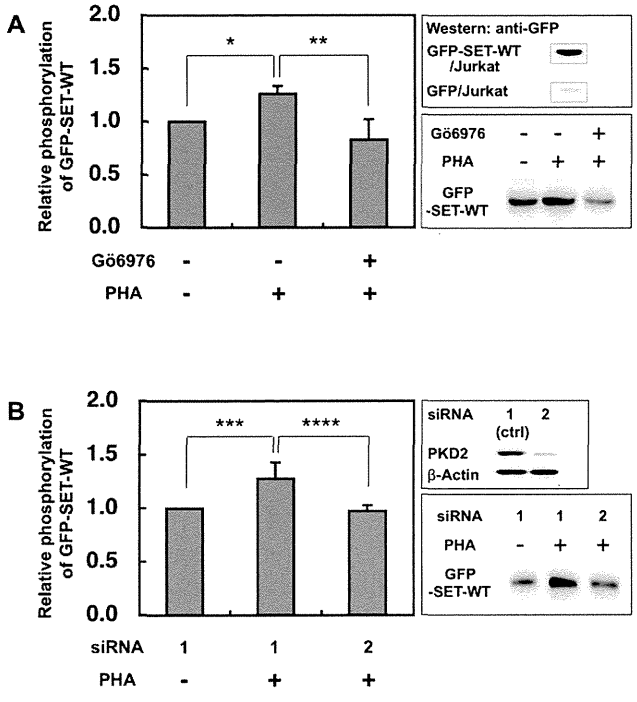

Figure 2. PKD2 is involved in the up-regulation of SET phoshorylation in activated Jurkat cells. (A) After Jurkat cells expressing GFP-SET were stimulated by PHA (2 μg/ml) with or without Gö6976 (3 μM), the phosphorylated GFP-tagged SET was collected by PhosphoProtein Purification kit and separated by SDS-PAGE. The phosphoprotein was transferred onto the PVDF membrane and quantified by ECL using anti-GFP antibody and the secondary antibody. The typical blot was shown in the lower-right panel. The luminescence of samples from cells without both stimulation and the inhibitor was assigned to be 1. The results were expressed as mean +SD for three independent experiments. *, $p<0.01$; **, $p<0.05$. As shown in the upper-right panel, phosphorylated GFP was not detected from the eluate of the PHA stimulated Jurkat cells expressing GFP only. (B) Jurkat cells expressing GFP-SET treated with control (ctrl) siRNA1 had no effect on the PKD2 expression, while siRNA2 markedly reduced the PKD2 expression (upper-right panel). The typical blot was shown in the lower-right panel. The luminescence of the samples from non-stimulated and siRNA1-treated cells was assigned to be 1. The results were expressed as mean +SD for three independent experiments. ***, $p<0.05$; ****, $p<0.05$, as determined by Student's *t* test.
doi:10.1371/journal.pone.0051242.g002

SET protein (MW = 32kd, pI = 4.1) in a faint protein spot (Fig. 1C, indicated by asterisks) overlapping to the specifically incorporated ^{32}P radioactivity. The detection of SET as a potential PKD2 substrate was in accordance with our previous observation where the SET protein was enriched in the bound fraction of PhosphoProtein Purification Column (Qiagen) applied with lysate of Jurkat cells over-expressing constitutively active PKD2 [12]. These observations supported the idea that SET protein was phosphorylated by activated PKD2 in Jurkat cells upon TCR stimulation.

PKD2 is involved in activation-induced up-regulation of SET phosphorylation in Jurkat cells

To monitor the amount of phosphorylated SET *in vivo*, Jurkat cells expressing GFP-SET-WT were stimulated with PHA and phospho-GFP-SET-WT (GFP-pSET-WT) was recovered and quantified by western blot using anti-GFP antibody as described in the Method section. The amount of GFP-pSET-WT was up-regulated after stimulation (Fig. 2), however, the up-regulation was compromised in the presence of PKD2 inhibitor Gö6976 (Fig. 2A). Knockdown of PKD2 by siRNA also reduced the up-regulation of GFP-pSET-WT induced by PHA stimulation (Fig. 2B). GFP only expressed in Jurkat cells was not phosphorylated by the PHA stimulation since GFP band was not detected (Fig. 2A upper right panel). These data suggest that PKD2 is involved in the phosphorylation of SET in the stimulated Jurkat cells.

PKD2 phosphorylates Ser171 of SET protein

To identify the Ser/Thr residues of SET phosphorylated by PKD2, we produced a series of recombinant 6×His-tagged SET proteins with various Ser/Thr to Ala substitutions and they were subjected to *in vitro* PKD2 kinase assay (Fig. 3). Phosphorylation of the C-terminal half portion (amino acid (aa) residues 128–277) of SET protein by constitutively-active (CA) PKD2 was higher than that of the N-terminal half portion (aa residues 1–132) (Fig. 3A, CA of N-half 1-132WT and C-half 128-277WT). Therefore, we focused our investigation on the C-terminal portion of SET. In this portion, there are 16 Ser/Thr residues (Fig. 3B). Introduction of Ser/Thr to Ala substitutions in aa residues148–156 region (Ser148, Ser152, Ser153, Ser155, Thr156 to Ala) and in 188–197 region (Ser188, Thr191, Thr194, Ser197 to Ala) did not affect the incorporation of ^{32}P radioactivity (Fig. 3A, CA C-half 148-156S-A and C-half 188-197ST-A). On the other hand, all Ser/Thr except for Ser162 and Ser178 to Ala substitutions abolished incorporation of ^{32}P radioactivity (Fig. 3A, CA C-half All ST-A (exS162, S178)). These data suggested that the possible phosphorylation sites were either Ser140, Thr167, Ser170, Ser171 or Thr173 in the C-terminal half portion. Among these Ser/Thr residues, Ser171 fitted to the putative PKD1 phosphorylation motif (LxK/RxxS) [24,25,26] and Ser171 to Ala substitution abrogated the phosphorylation as well as the all Ser/Thr to Ala mutant did (Fig. 3A, CA C-half S171A and C-half All ST-A). Therefore, it turned out that Ser171 of SET protein was phosphorylated by active PKD2 *in vitro*. Since all ST-A mutant protein did not incorporate the radioactivity, the Ser/Thr residues present in the vector-derived amino acid residues were not likely to be phosphorylated by PKD2.

To examine whether Ser171 is involved in SET phosphorylation *in vivo*, Jurkat cells expressing GFP-tagged SET with Ser171 to Ala mutant (GFP-SET-S171A) were stimulated with PHA in the absence or presence of PKD2 inhibitor Gö6976 and the amount of phospho-GFP-SET-S171A recovered from each cell lysate was compared by the western blotting using anti-GFP antibody. Contrary to the data shown in Fig. 2, the amount of phospho-GFP-SET-S171A was unchanged by the stimulation in the absence or presence of PKD2 inhibitor, suggesting that SET Ser171 is the major phosphorylation site of PKD2 activated by TCR stimulation (Fig. 4).

Substitution of Ser171 to Glu in SET compromised its inhibitory effect on PP2A phosphatase activity

Since SET protein is known to be a natural inhibitor for PP2A [2], we next tried to ask the effect of Ser171 phosphorylation on its inhibitory activity for PP2A. For this purpose, we prepared recombinant wild-type SET (SET-WT), phosphorylation-mimic Ser171 to Glu (S171E) and non-phosphorylation-mimic Ser171 to Ala (S171A) mutants. Equal amount of each purified recombinant SET protein was added to the PP2A phosphatase reaction mixture where PKA-labeled ^{32}P-MBP was used as a substrate. As shown in Fig. 5, the phosphatase activity of PP2A was dose-dependently inhibited by the addition of the SET proteins. However, we noticed that the phosphorylation-mimic S171E mutant was less

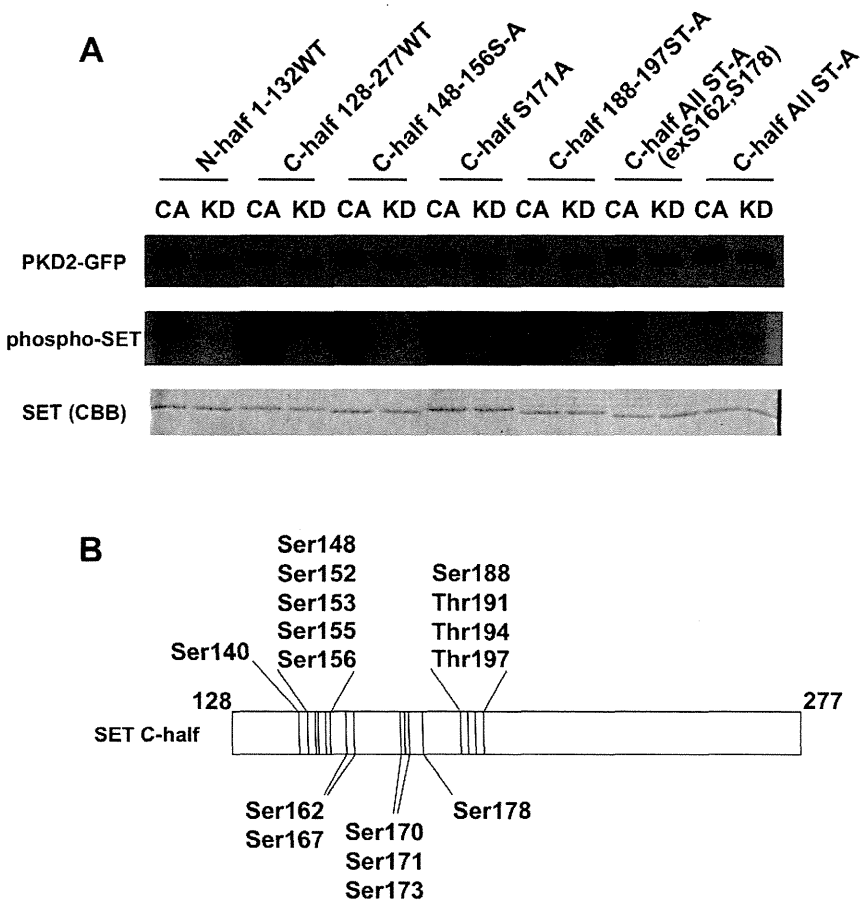

Figure 3. Ser171 of SET is phosphorylated by PKD2. (A) The indicated 6×His-tag SET mutant proteins were treated with immunoprecipitated constitutively active-PKD2-GFP (CA) or kinase dead-PKD2-GFP (KD) in the presence of [γ-^{32}P]-ATP. The kinase assay mixture was analyzed with SDS-PAGE. Immunoprecipitated PKD2-GFP was blotted with anti-GFP antibody (upper panel) to monitor equal loading of the PKD2 mutants. Phosphorylation of the SET mutants was monitored by incorporated radioactivity (middle panel). Equal loading of each SET mutant protein was confirmed by staining with Coomassie Brilliant Blue (CBB, lower panel). The data shown are representative results from three independent experiments with similar results. (B) A diagram of Ser/Thr residues present in C-terminal half (128–277) of SET protein.
doi:10.1371/journal.pone.0051242.g003

inhibitory than S171A or SET-WT. Even at the highest concentration (400 nM) of SET proteins tested, PP2A retained its phosphatase activity in samples with SET-S171E while that in samples with SET-S171A or SET-WT was completely abolished (Fig. 5).

Suppression of PKD2 activity retains higher phosphorylation status of Tyr307 of PP2A

The data presented above suggested the possibility that PKD2 may regulate PP2A activity through SET phosphorylation *in vivo*. To ask this possibility, the relationship between PKD2 and activity of PP2A in *ex vivo* system was investigated using a TCR stimulated human CD4$^+$ T cell clone or Jurkat cells. Since it is reported that phosphorylation status of Tyr307 of PP2A catalytic subunit inversely correlates with the activity of PP2A [22], we monitored phospho-Tyr307 of PP2A from stimulated T cells or Jurkat cells (Fig. 6).

The human CD4$^+$ T cell clone was stimulated by co-culturing with mouse L cells expressing its cognate TCR-ligand, HLA-DR4 covalently-linked with the antigenic peptide [19], under the presence or absence of PKD2 inhibitor Gö6976 (3 μM). Jurkat cells of which PKD2 expression was knocked down by RNAi were stimulated with anti-CD3ε antibody plus the second antibody. The phosphorylation status of Tyr307 of PP2A was reduced in a time-dependent manner after TCR stimulation in both human CD4$^+$ T cell clone without inhibitor (Fig. 6A, open symbols) and Jurkat cells treated with control siRNA (Fig. 6B, open symbols), suggesting that the PP2A phosphatase activity was up-regulated after TCR stimulation. On the other hand, the human CD4$^+$ T cell clone treated with the PKD2 inhibitor (Fig. 6A, closed symbols) and PKD2-knocked down Jurkat cells by the siRNA (Fig. 6B, closed symbols) retained higher phosphorylation levels of PP2A compared with those of the control cells since PKD2 up-regulates PP2A activity after TCR stimulation possibly through SET phosphorylation. In accordance with this notion, stimulated Jurkat cells overexpressing GFP-SET-S171A (Fig. 6C, western blot in the upper box and closed circles) showed higher phosphorylation status of PP2A Tyr307 than that of the control Jurkat cells (Fig. 6C, open circles) at all the time points analyzed.

Overexpression of GFP-SET-S171A down-regulates ERK activity

Chen et al. reported that knockdown of endogenous PKD2 down-regulated ERK activity in cancer cells [27]. It has been also reported that PP2A dephosphorylates the inhibitory phosphate at Ser259 of Raf-1, and thus PP2A activates Raf-1 and then activates

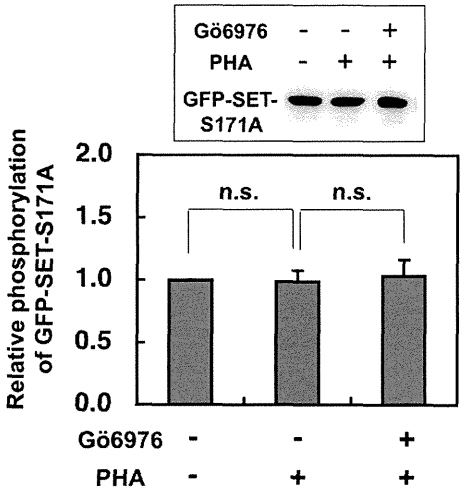

Figure 4. Phospho-GFP-SET-S171A levels in Jurkat were unchanged by PHA stimulation with or without PKD2 inhibitor. The Jurkat cells expressing GFP-SET-S171A were stimulated and phosphorylation status of GFP-SET-S171A was investigated by the same method as described in Fig. 2. The results were indicated as mean +SD for three independent experiments. There was no significant up- or down-regulation of recovered phospho-GFP-SET-S171A by PHA stimulation with or without PKD2 inhibitor, suggesting that Ser171 of SET is the major target site of TCR-activated PKD2.
doi:10.1371/journal.pone.0051242.g004

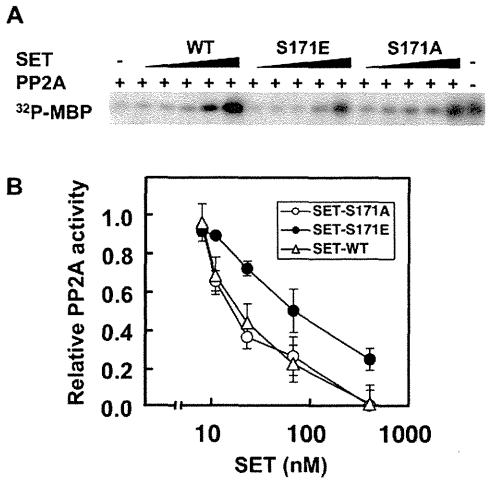

Figure 5. Substitution of Ser171 to Glu (SET-S171E) in SET compromised its inhibitory effect on PP2A. Substitution of Ser171 to Glu (SET-S171E), which mimics phosphorylated SET at Ser171 residue, reduced its inhibitory effect on PP2A compared with Ser171 to Ala substitution (SET-S171A) or wild-type SET did. (A) The phosphatase activity of PP2A (37 μU) under the presence of indicated concentration of recombinant SET was monitored by using ^{32}P-labeled MBP as a substrate. After SET proteins and PP2A were preincubated for 15 min at 4°C, ^{32}P-MBP was added and incubated for 10 min at 37°C. The reaction mixture was separated with SDS-PAGE. The inhibitory effect of SET proteins on PP2A activity was visualized by exposing the SDS-PAGE gel with PP2A-treated ^{32}P-MBP to X-ray film. The data shown are representative results from three independent experiments with similar results. (B) The relative PP2A activity to the radioactivity of ^{32}P-MBP without SET (assigned to be 1) was calculated from the radioactivity of MBP bands in the dried gel shown in (A). Values represent the means ±SD from three independent experiments.
doi:10.1371/journal.pone.0051242.g005

ERK-dependent signaling pathway [28,29,30,31,32]. To ask whether SET is involved in the ERK phosphorylation, we compared ERK phosphorylation in Jurkat cells overexpressing GFP-SET-S171A (Fig. 6C, upper box) with that in normal Jurkat cells after stimulation (Fig. 7). Jurkat cells overexpressing GFP-SET-S171A showed slightly but significantly lower phospho-ERK/ERK ratio compared with that of the Jurkat cells, suggesting that overexpression of non-phosphorylation-mimic SET compromised PP2A activity (Fig. 6C), which resulted in the down-regulation of ERK activation in the stimulated Jurkat cells.

Discussion

The phosphoprotein SET has been shown to have various functions in cellular activities [1,2,3,33,27,34]. However, the relation between the phosphorylation status of SET and its functions has still been investigated. In this work, we mapped one of the phosphorylation sites for PKD2 at Ser171 of SET. Substitution of Ser171 to Glu resulted in reduction of its inhibitory effect on phosphatase activity of PP2A and overexpression of non-phosphorylation-mimic S171A SET resulted in reduction of PP2A activity.

Since the all Ser/Thr to Ala mutant of C-terminal half of 6×His-tag SET protein was not phosphorylated by PKD2, Ser/Thr residues present in the linker portion between 6×His-tag and SET were not target phosohorylation sites for PKD2. This suggested that there must be other target phosohorylation sites of PKD2 in the N-terminal half of SET protein since it also incorporated the ^{32}P radioactivity when treated with active PKD2 and the sites remain to be mapped. However, since the phosphorylation of N-terminal half was much weaker than that of the C-terminal half portion, the PKD2 phosphorylation sites in the N-terminal half portion do not seem to be as effectively phosphorylated by PKD2 as Ser171. In addition, the amino acid sequences preceding Ser171 (LTKRSS) fits to the phosphorylation motif of PKD1 (LxR/KxxS) [24,25,26] and the LTKRSS sequence is conserved among the SET proteins of various species such as calf, chicken, mouse, xenopus and human, suggesting the functional importance of this amino acid sequence. Furthermore, Ser171 is positioned in the bottom surface of the predicted earmuff structure of SET [34]. This is in accordance with the accessibility of the kinase for phosphorylation and would provide the interaction site with other molecules such as PP2A.

The interaction between SET and PKD2 was shown in Jurkat cells since the anti-PKD2 antibody co-immunoprecipitated SET from the Jurkat cell lysate (Supporting Information S1). However, in the reciprocal experiment, the anti-SET antibody did not co-immunoprecipitate PKD2. One possibility for this discrepancy may be due to the overlapping binding site on SET for the anti-SET antibody and PKD2. Supporting this, the anti-GFP antibody co-immunoprecipitated PKD2 from GFP-SET-WT-expressing Jurkat cells together with GFP-SET (Supporting Information S1). Although we tried to show the SET phosphorylation by PKD2 in primary human T cells by *in vivo* ^{32}P –labeling of SET, *ex vivo* detection of phosphorylated SET by anti-phospho-Ser antibody or by the Phos-tag detection kit (FMS Laboratory, Hiroshima, Japan), the clear difference of the phosphorylation status of SET before and after stimulation was not observed at this moment.

SET is a multi-functional protein and has an acidic domain rich in Glu and Asp residues at its very C-terminus (amino acid positions 224–277). The acidic domain is indispensable for its inhibitory effect on the histone acetyltransferases [1] and on the nucleosome assembly protein activity [35], however, the experiment using truncated mutants of SET showed that the inhibitory

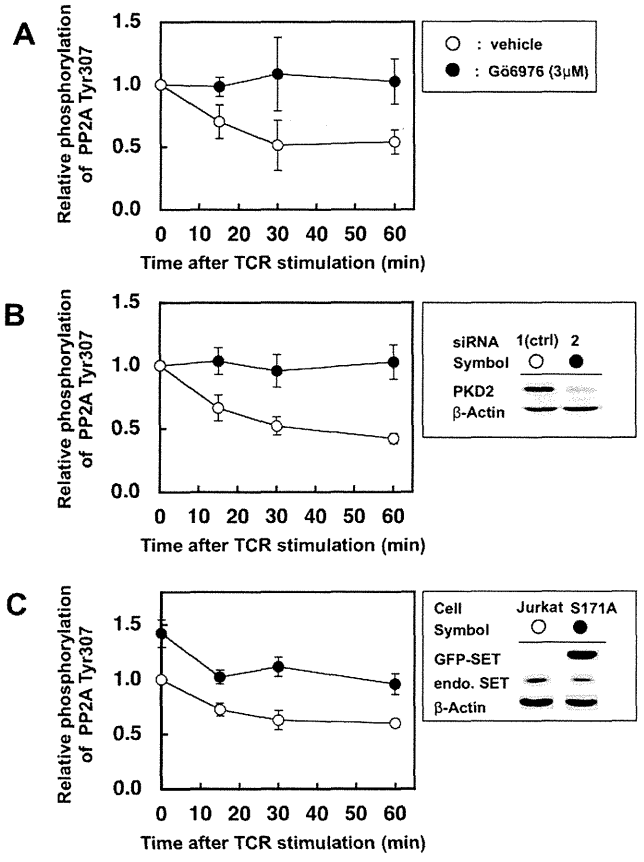

Figure 6. Suppression of PKD2 up-regulates Tyr307 phosphorylation of PP2A catalytic subunit after TCR stimulation. (A) Human $CD4^+$ T cell clone was stimulated by L cells expressing its cognate ligands in the presence (closed circles) or absence (open circlse) of PKD2 inhibitor Gö6976 (3 μM). (B) Jurkat cells treated with siRNA were stimulated by anti-CD3ε antibody and anti-mouse IgG antibody. Treatment with siRNA2 (closed circles) significantly reduced the PKD2 expression, while siRNA1 (open circles) had almost no effect and hence used as negative controls (right panel). (C) Normal Jurkat cells (open circles) and Jurkat cells expressing GFP-SET-S171A (closed circles) were stimulated by anti-CD3ε antibody and anti-mouse IgG antibody. The latter cells expressed 4.5-fold higher GFP-SET-S171A than the endogenous SET as judged by the intensity of the bands using anti-SET antibody on the Western blot (upper box). Cell lysate were subjected to SDS-PAGE followed by western blot using anti-PP2A phospho-Tyr307 antibody and horseradish peroxidase-conjugated second antibody. The amount of each band was quantified by using ECL and LAS-4000. The same membrane was stripped and reprobed with the anti-PP2A C-subunit antibody to monitor relative abundance of total PP2A protein. Values represent the means ±SD from three independent experiments.
doi:10.1371/journal.pone.0051242.g006

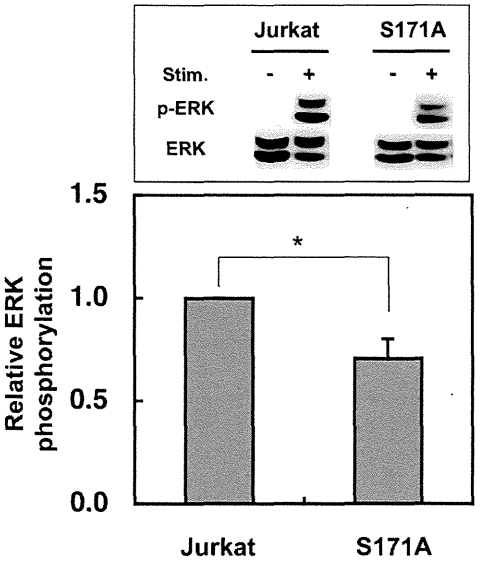

Figure 7. Overexpression of GFP-SET-S171A reduced the ERK activation after stimulation. Normal and GFP-SET-S171A-overexpressing Jurkat cells were stimulated by anti-CD3e antibody and anti-mouse IgG antibody for 7 min were lyzed and subjected to SDS-PAGE followed by the western blot analyses. The phospho-ERK (p-ERK) was first detected and quantified and after stripping off the antibodies, ERK1 was detected and quantified to monitor p-ERK/ERK1 ratio. The p-ERK/ERK1 ratio of Jurkat cell was assigned to be 1. The results were indicated as mean +SD for three independent experiments. *, $p<0.01$, as determined by Student's *t* test.
doi:10.1371/journal.pone.0051242.g007

activity of SET toward PP2A resides in the N-terminal amino acid region of 26–119 [36]. Therefore, phosphorylation of Ser171 by PKD2 seems to regultae the inhibitory activity from outside of the N-terminal regions of SET. Recently, Vera et al. reported that casein kinase 2 (CK2) was one of the SET binding proteins and phosphorylated SET *in vitro* [37]. Although the phosphorylation sites of SET by CK2 were not identified, they speculated that phosphorylation of SET by CK2 might regulate its proteolytic degradation and cytosol-nuclear shuttling since CK2 phosphorylation of necleosome assembly protein-1, a structurally and functionally similar protein to SET, was reported to have such functions as SET did [38]. Collectively, phosphorylation of SET by kinases may regulate some of the SET functions.

The *in vitro* phosphatase assay using immunoprecipitated PP2A from activated T cells by colorimetric assays using *p*-nitrophenol or Malachite Green [39], or by the MBP-based radioactive assay were fluctuated and thus not reliable. Therefore, we adopted to monitor phosphorylation status of Tyr307 of PP2A, which inversely correlate with the phosphatase activity [22]. This method was also adopted by Neviani et al. and they reported that phosphorylation of tyrosine 307 of PP2A was increased in Bcr-Abl^+ cells by over-expressing SET protein [40]. Without PKD2-specific inhibitor or reduction of PKD2 by RNAi, the amount of PP2A phospho-Tyr307 was decreased in time-dependent manner, suggesting the increase of PP2A activity after TCR-stimulation. Actually, phosphatase activity of immunoprecipitated PP2A from anti-CD3ε antibody stimulated Jurkat cells was up-regulated compared to that of non-stimulated cells (Supporting Information S2). This reduction of phospho-Tyr307 of PP2A was compromised by the suppression of PKD2 activity by either its specific inhibitor or RNAi, showing a relation between the PKD2 activity and some PP2A status, possibly through the phosphorylation of the natural PP2A inhibitor SET. Further such investigations using anti-phospho-Ser171 of SET should be necessary to confirm the hypothesis in the near future.

There are many reports providing the evidences that PP2A dephosphorylates the inhibitory phosphate at Ser259 of Raf-1, and thus PP2A activates Raf-1 and then activates ERK-dependent signaling pathway [28,29,30,31,32] and knocking down of PKD2 resulted in the decrease of the ERK activation in LNCaP prostate cancer cells [27]. Although we have no direct evidence at this time concerning the relation among SET phosphorylation by PKD2, up-regulation of PP2A and ERK activities *in vivo*, overexpression of

non-phosohorylation-mimic mutant of SET in TCR-stimulated Jurkat cells resulted in the down-regulation of ERK phosphorylation as well as PP2A activity, suggesting the involvement of phosphorylation status of SET and PP2A activity in the ERK activation. Together, it is tempting to hypothesize that PKD2 is a positive regulator of T cell activation through SET phosphorylation and up-regulation of PP2A activity, which results in the activation of MAPK pathway. This notion is in accordant with our first finding that partially-agonistic TCR ligands induced ZAP-70 independent T cell proliferation and interferon-γ production, which was completely suppressed by PKD2 inhibitor [9], since PKD2 is activated by the over-expressed partially agonistic TCR ligands and induces T cell activation through the "SET phosphorylation-PP2A activation-ERK activation" pathway, which skips ZAP-70 activation.

In conclusion, the roles of PKD2 and its substrate SET in T cell activation were investigated and we found that PKD2 phosphorylates Ser171 of SET, which resulted in the reduction of its inhibitory effect on PP2A phosphatase activity.

Supporting Information

Supporting Information S1 Co-immunoprecipitation of SET by anti-PKD2 antibody from Jurkat cells lysate. Jurkat cells (1×10^7) and GFP-SET-WT expressing Jurkat cells (1×10^7) were stimulated with PMA (20 ng/ml) and ionomycin (2 μg/ml) for 30 min at 37°C and lysed. Each cell lysate was immunoprecipitated with anti-PKD2, anti-SET or anti-GFP antibodies and Protein A beads. The anti-PKD2 antibody co-immunoprecipitated SET (left pannels) from Jurkat cell lysate. Reciprocally, the anti-SET antibody failed to co-immunoprecipitate PKD2 from Jurkat cell lysate (middle panels), while the anti-GFP antibody could co-immunoprecipitate PKD2 (right pannels) with GFP-SET.
(TIF)

Supporting Information S2 PP2A phosphatase activity was up-regulated after TCR stimulation in Jurkat cells. Jurkat cells (1×10^6) were left untreated or stimurated with anti-CD3ε antibody and anti-mouse IgG antibody for 30 min. Each cell lysate was immunoprecipitated with anti-PP2A C-subunit antibody (anti-PP2A) or non-specific control antibody (IgG) and Protein A beads. The immunocomplex were incubated with ^{32}P-MBP as a substrate. The reaction mixture was separated with SDS-PAGE. The autoradiogram was shown in the upper panel. The phosphatase activity was measured as a remaining radioactivity of ^{32}P-MBP. The radioactivity of ^{32}P-MBP treated with the immune complex precipitated with non-specific control antibody was assigned to be 1 (lower panel). Student's t test analysis for the PP2A activity of stimulated versus non-stimulated was done. *, $p<0.01$ (n = 4).
(TIF)

Acknowledgments

We are grateful to Dr. H. Miyoshi for donating us the vectors for lentiviral gene expression.

Author Contributions

Conceived and designed the experiments: AI. Performed the experiments: AI KH. Analyzed the data: AI KH NA YN. Contributed reagents/materials/analysis tools: AI KH. Wrote the paper: AI.

References

1. Seo SB, McNamara P, Heo S, Turner A, Lane WS, et al. (2001) Regulation of histone acetylation and transcription by INHAT, a human cellular complex containing the set oncoprotein. Cell 104: 119–130.
2. Li M, Makkinje A, and Damuni Z (1996) The myeloid leukemia-associated protein SET is a potent inhibitor of protein phosphatase 2A. J Biol Chem 271: 11059–11062.
3. Fan Z, Beresford PJ, Oh DY, Zhang D, Lieberman J (2003) Tumor suppressor NM23-H1 is a granzyme A-activated DNase during CTL-mediated apoptosis, and the nucleosome assembly protein SET is its inhibitor. Cell 112: 659–672.
4. Millward TA, Zolnierowicz S, Hemmings BA (1999) Regulation of protein kinase cascades by protein phosphatase 2A. Trends Biochem Sci 24: 186–191.
5. Zolnierowicz S (2000) Type 2A protein phosphatase, the complex regulator of numerous signaling pathways. Biochem Pharmacol 60: 1225–1235.
6. Rykx A, De Kimpe L, Mikhalap S, Vantus T, Seufferlein T, et al. (2003) Protein kinase D: a family affair. FEBS Lett 546: 81–86.
7. Matthews SA, Iglesias T, Rozengurt E, Cantrell D (2000) Spatial and temporal regulation of protein kinase D (PKD). EMBO J 19: 2935–2945.
8. Marklund U, Lightfoot K, Cantrell D (2003) Intracellular location and cell context-dependent function of protein kinase D. Immunity 19: 491–501.
9. Irie A, Chen YZ, Tsukamoto H, Jotsuka T, Masuda M, et al. (2003) Unique T cell proliferation associated with PKCμ activation and impaired ZAP-70 phosphorylation in recognition of overexpressed HLA/partially agonistic peptide complexes. Eur J Immunol 33: 1497–1507.
10. Parra M, Kasler H, McKinsey TA, Olson EN, Verdin E (2005) Protein kinase D1 phosphorylates HDAC7 and induces its nuclear export after T-cell receptor activation. J Biol Chem 280: 13762–13770.
11. Dequiedt F, Van Lint J, Lecomte E, Van Duppen V, Seufferlein T, et al. (2005) Phosphorylation of histone deacetylase 7 by protein kinase D mediates T cell receptor-induced Nur77 expression and apoptosis. J Exp Med 201: 793–804.
12. Irie A, Harada K, Tsukamoto H, Kim JR, Araki N, et al. (2006) Protein kinase D2 contributes to either IL-2 promoter regulation or induction of cell death upon TCR stimulation depending on its activity in Jurkat cells. Int Immunol 18: 1737–1747.
13. von Blume J, Knippschild U, Dequiedt F, Giamas G, Beck A, et al. (2007) Phosphorylation at Ser244 by CK1 determines nuclear localization and substrate targeting of PKD2. EMBO J 26: 4619–4633.
14. Matthews SA, Navarro MN, Sinclair LV, Emslie E, Feijoo-Carnero C, et al. (2010) Unique functions for protein kinase D1 and protein kinase D2 in mammalian cells. Biochem J 432: 153–163.
15. Matthews SA, Liu P, Spitaler M, Olson EN, McKinsey TA, et al. (2006) Essential Role for Protein Kinase D Family Kinases in the Regulation of Class II Histone Deacetylases in B Lymphocytes. Mol Cell Biol 26: 1569–1577.
16. Liu P, Scharenberg AM, Cantrell DA, Matthews SA (2007) Protein kinase D enzymes are dispensable for proliferation, survival and antigen receptor-regulated NFκB activity in vertebrate B-cells. FEBS Lett 581: 1377–1382.
17. Ren M, Feng H, Fu Y, Land M, Rubin CS (2009) Protein kinase D is an essential regulator of *C. elegans* innate immunity. Immunity 30: 521–532.
18. Zheng H, Qian J, Varghese B, Baker DP, Fuchs S (2011) Ligand-stimulated downregulation of the α interferon receptor: role of protein kinase D2. Mol Cell Biol 31: 710–720.
19. Chen YZ, Matsushita S, Nishimura Y (1996) Response of a human T cell clone to a large panel of altered peptide ligands carrying single residue substitutions in an antigenic peptide: characterization and frequencies of TCR agonism and TCR antagonism with or without partial activation. J Immunol. 157: 3783–3790.
20. Kim JR, Irie A, Tsukamoto H, Nishimura Y (2006) A role of kinase inactive ZAP-70 in altered peptide ligand stimulated T cell activation. Biochem Biophys Res Commun 341: 19–27.
21. Tsukamoto H, Irie A, Chen YZ, Takeshita K, Kim JR, et al. (2006) TCR ligand avidity determines the mode of B-Raf/Raf-1/ERK activation leading to the activation of human $CD4^+$ T cell clone. Eur J Immunol 36: 1926–1937.
22. Chen J, Martin BL, Brautigan DL (1992) Regulation of protein serine-threonine phosphatase type-2A by tyrosine phosphorylation. Science 257: 1261–1264.
23. Gschwendt M, Dieterich S, Rennecke J, Kittstein W, Mueller HJ, et al. (1996) Inhibition of protein kinase Cμ by various inhibitors. Differentiation from protein kinase C isoenzymes. FEBS Lett 392: 77–80.
24. Nishikawa K, Toker A, Wong K, Marignani PA, Johannes FJ, et al. (1998) Association of protein kinase Cμ with type II phosphatidylinositol 4-kinase and type I phosphatidylinositol-4-phosphate 5-kinase. J Biol Chem 273: 23126–23133.
25. Hutti JE, Jarrell ET, Chang JD, Abbott DW, Storz P, et al. (2004) A rapid method for determining protein kinase phosphorylation specificity. Nat Methods 1: 27–29.
26. Doppler H, Storz P, Li J, Comb MJ, Toker A (2005) A phosphorylation state-specific antibody recognizes Hsp27, a novel substrate of protein kinase D. J Biol Chem 280: 15013–15019.
27. Chen J, Giridhar KV, Zhang L, Xu S, Wang QJ (2011) A protein kinase C/protein kinase D pathway protects LNCaP prostate cancer cells from phorbol

ester-induced apoptosis by promoting ERK1/2 and NF-κB activities. Carcinogenesis 32: 1198–1206.
28. Abraham D, Podar K, Pacher M, Kubicek M, Welzel N, et al. (2000) Raf-1-associated protein phosphatase 2A as a positive regulator of kinase activation. J Biol Chem 275: 22300–22304.
29. Jaumot M, Hancock JF (2001) Protein phosphatases 1 and 2A promote Raf-1 activation by regulating 14-3-3 interactions. Oncogene 20: 3949–3958.
30. Kubicek M, Pacher M, Abraham D, Podar K, Eulitz M, et al. (2002) Dephosphorylation of Ser-259 regulates Raf-1 membrane association. J Biol Chem 277: 7913–7919.
31. Adams DG, Coffee RL Jr, Zhang H, Pelech S, Strack S, et al. (2005) Positive regulation of Raf1-MEK1/2-ERK1/2 signaling by protein serine/threonine phosphatase 2A holoenzymes. J Biol Chem 280: 42644–42654.
32. Chetoui N, Gendron S, Chamoux E, Aoudjit F (2006) Collagen type I-mediated activation of ERK/MAP Kinase is dependent on Ras, Raf-1 and protein phosphatase 2A in Jurkat T cells. Mol Immunol 43: 1687–1693.
33. Estanyol JM, Jaumot M, Casanovas O, Rodriguez-Vilarrupla A, Agell N, et al. (1999) The protein SET regulates the inhibitory effect of p21(Cip1) on cyclin E-cyclin-dependent kinase 2 activity. J Biol Chem 274: 33161–33165.
34. Muto S, Senda M, Akai Y, Sato L, Suzuki T, et al. (2007) Relationship between the structure of SET/TAF-Iβ/INHAT and its histone chaperone activity. Proc Natl Acad Sci U S A 104: 4285–4290.
35. Beresford PJ, Zhang D, Oh DY, Fan Z, Greer EL, et al. (2001) Granzyme A activates an endoplasmic reticulum-associated caspase-independent nuclease to induce single-stranded DNA nicks. J Biol Chem 276: 43285–43293.
36. Saito S, Miyaji-Yamaguchi M, Shimoyama T, Nagata K (1999) Functional domains of template-activating factor-I as a protein phosphatase 2A inhibitor. Biochem Biophys Res Commun 259: 471–475.
37. Vera J, Estanyol JM, Canela N, Llorens F, Agell N, et al. (2007) Proteomic analysis of SET-binding proteins. Proteomics 7: 578–587.
38. Li M, Strand D, Krehan A, Pyerin W, Heid H, et al. (1999) Casein kinase 2 binds and phosphorylates the nucleosome assembly protein-1 (NAP1) in *Drosophila melanogaster*. J Mol Biol 293: 1067–1084.
39. Harder KW, Owen P, Wong LK, Aebersold R, Clark-Lewis I, et al. (1994) Characterization and kinetic analysis of the intracellular domain of human protein tyrosine phosphatase β (HPTPβ) using synthetic phosphopeptides. Biochem J 298 (Pt 2): 395–401.
40. Neviani P, Santhanam R, Trotta R, Notari M, Blaser BW, et al. (2005) The tumor suppressor PP2A is functionally inactivated in blast crisis CML through the inhibitory activity of the BCR/ABL-regulated SET protein. Cancer Cell 8: 355–368.

ANTICANCER RESEARCH *33*: 153-160 (2013)

Proteomic Analysis Showed Down-regulation of Nucleophosmin in Progressive Tumor Cells Compared to Regressive Tumor Cells

TAKANORI TAKENAWA[1], YASUHIRO KURAMITSU[2], YUFENG WANG[2], FUTOSHI OKADA[3], KAZUHIRO TOKUDA[2], TAKAO KITAGAWA[2], YOSHIYA UEYAMA[1] and KAZUYUKI NAKAMURA[2]

Departments of [1]Oral and Maxillofacial Surgery, and [2]Biochemistry and Functional Proteomics, Yamaguchi University Graduate School of Medicine, Ube, Yamaguchi, Japan;
[3]Department of Molecular and Cellular Biology, Tottori University School of Life Sciences, Yonago, Japan

Abstract. *Important strategies against cancer are based on the understanding of the mechanisms of tumor progression. To elucidate alterations regarding tumor progression, we have performed proteomic differential display analysis for the expression of intracellular proteins in the regressive murine fibrosarcoma cell clone QR-32 and the progressive malignant tumor cell clone QRsP-11, derived from QR-32, by means of combination of two-dimensional gel electrophoresis (2-DE) and liquid chromatography-tandem mass spectrometry (LC-MS/MS), and we have previously reported on relevant results. However, besides the protein spots which we already reported, we identified three more particular spots of interest. In the present study, two-dimensional western blot analysis demonstrated a significantly lower expression of three isoforms of nucleophosmin in progressive, compared to regressive cell clones. These results suggest that the down-regulation of the identified nucleophosmin proteins in QRsP-11 cells compared to QR-32 cells is possibly related to tumor malignant progression.*

The most crucial features of malignant tumors are unpredictable development and progression. Progressive tumor cells show rapid growth, unrestricted proliferation activity, serious invasiveness and disorderly metastatic capacity, compared to regressive benign tumor cells. Okada *et al.* have established progressive and regressive murine fibrosarcoma tumor models (QR-32 clone and QRsP-11 clone) (1, 2). The regressive clone QR-32 is a weakly tumorigenic and non-metastatic cell clone. The progressive clone QRsP-11, on the other hand, is a progressive malignant tumor cell clone derived from QR-32. After injection of 1×10^6 cells intravenously, or up to 2×10^5 cells subcutaneously, in normal syngeneic mice, QR-32 cells regress spontaneously. However, when they are subcutaneously co-implanted with gelatin sponge, they grow progressively. After these progressively-growing cells were established as cell lines (QRsP), they had the ability to progressively grow in mice, even in the absence of gelatin sponge. The characteristic feature of QRsPs as malignant tumor cell clones is that they are more tumorigenic and metastatic, and QRsP-11 is one such QRsP clone.

The aim of this study was to identify the differentially expressed proteins between the clones QR-32 and QRsP-11. The comparison of the differential expression of proteins between benign tumor cells of single-cell origin and their derived malignant tumor cells is beneficial in detecting various important factors in inflammation-associated tumor progression. We have reported many proteomic studies of QR-32 and QRsP-11 cells by using two-dimensional gel electrophoresis (2-DE) (3-5). The differential display analysis for the expression of nuclear proteins between QR-32 and QRsP-11 showed eight nuclear proteins to be differentially-regulated, including zing finger protein ZXDC, in QRsP-11 compared with QR-32 cells (4). The proteomic differential display analysis for the expression of cytoplasmic proteins in QR-32 and QRsP-11 cells showed 11 spots for differentially regulated proteins, including heat-shock protein (HSP)-90 in QRsP-11 compared with QR-32 cells (3). Our recent 2-DE analysis of QR-32 and QRsP-11 cells showed three spots for down-regulated proteins in the progressive malignant tumor cell clone QRsP-11, compared to QR-32 cells, which were not identified in previous studies. Liquid chromatography-tandem mass spectrometry (LC-MS/MS) identified these

Correspondence to: Yasuhiro Kuramitsu, MD, Ph.D., Department of Biochemistry and Functional Proteomics, Yamaguchi University Graduate School of Medicine, 1-1-1 Minami-kogushi, Ube, Yamaguchi 755-8505, Japan. Tel: +81 836222213, Fax: +81 836222212, e-mail: climates@yamaguchi-u.ac.jp

Key Words: Two-dimentional gel electrophoresis, LC-MS/MS, 2-D western blotting, nucleophosmin, tumor progression.

three spots as nucleophosmin. In the present study, we investigated these three spots by means of 2-D western blot analysis with an antibody against nucleophosmin.

Materials and Methods

Tumor cell lines and culture conditions. QR-32 and QRsP-11 are murine fibrosarcoma cell lines which were established at the Hokkaido University, the origin and characteristics of which have been previously described (1-6). Briefly, QR-32 cells are unable to grow when injected subcutaneously in C57Bl/6 mice and they spontaneously regress in syngeneic mice. QRsP-11 cells were obtained from the tumors which arose in mice after subcutaneous co-implantation of QR-32 cells with gelatin sponge, and show strong tumorigenicity. They were cultured in Eagle's minimum essential medium supplemented with 10% fetal bovine serum, sodium pyruvate, non-essential amino acids and L-glutamine, at 37°C. We used these cell lines passaged fewer than 10 times in culture after the cells had been sent to our laboratory from the Division of Cancer Pathobiology, Institute for Genetic Medicine, Hokkaido University, Sapporo, Japan.

Sample preparation. Cells were homogenized in lysis buffer [50 mM Tris-HCl (pH 7.5), 165 mM sodium chloride, 10 mM sodium fluoride, 1 mM sodium vanadate, 1 mM phenylmethylsulfonyl fluoride, 10 mM EDTA, 10 μg/ml aprotinin, 10 μg/ml leupeptin, and 1% NP-40] on ice. After centrifugation at 21,500 ×*g* for 30 min at 4°C, the supernatants were used for sample analysis (7).

Two-dimensional gel electrophoresis (2-DE). Eighty micrograms of protein were used for each 2-DE. For the first dimension, isoelectric focusing (IEF) was performed in an IPGphor 3 IEF unit (GE Healthcare, Chalfont St Giles, Buckinghamshire, UK) on 11 cm, immobilized, pH 3-10 linear gradient strips (Bio Rad, Hercules, CA, USA) at 50 μA/strip. Samples were dissolved in 200 μl of rehydration buffer [8 M urea, 2% CHAPS, 0.01% bromophenol blue, 1.2% Destreak reagent (GE Healthcare)] and loaded into the IPGphor strip holder (GE Healthcare). IEF was performed using the following voltage program: rehydration for 10 h (no voltage); a stepwise increase from 0 to 500 V for 4 h; 500 to 1,000 V for 1 h; 1,000 to 8,000 V for 4h; a linear increase from 8,000 V for 20 min, and a final phase of 500 V from 20,000 to 30,000 Vh. In the second dimension, sodium dodecyl sulfate-polyacrylamide gel electrophoresis (SDS-PAGE) was performed on a pre-cast polyacrylamide gel with a linear concentration gradient of 5-20% (Bio Rad), ran at 200 V (8).

Fluorescent gel staining. After 2-DE, the gels were washed with ultrapure water three times, and then fixed in 40% ethanol and 10% acetic acid solution for 2 h. The gels were stained with a fluorescent gel staining, Flamingo™ Fluorescent Gel Stain (Bio-Rad), overnight. Stained gels were washed with ultrapure water (Wako Pure Chemical Industries, Osaka, Japan) three times (9, 10).

Image analysis and spot picking. The gels were scanned using a ProEXPRESS 2D Proteomic Imaging System (Perkin Elmer, Waltham, MA, USA). Expression levels of the protein spots were quantified with the Progenesis SameSpot software (Nonlinear Dynamics Ltd., Newcastle upon Tyne, UK) (7, 9), and the differences in expression between QR-32 and QRsP-11 cells were analyzed statistically by ANOVA test, with $p<0.05$ being considered significant. Two-DE analysis was repeated three times. After statistical analysis, the gels were re-stained with See Pico™ (Benebiosis Co., Ltd, Seoul, Korea) (11), and the selected spots whose expression was significantly different between QRsP-11 and QR-32 cells were picked-up for MS analysis.

In-gel digestion. The See Pico™ dye was removed by washing three times in 60% methanol, 0.05 M ammonium bicarbonate, and 0.005 M DL-dithiothreitol (DTT) for 15 min. The sample in the gel piece was reduced twice in 50% acetonitrile (ACN), 0.05 M ammonium bicarbonate, and 0.005 M DTT for 10 min. The gel pieces were dehydrated twice in 100% ACN for 30 min and incubated with an in-gel digestion reagent containing 10 μg/ml sequencing-grade modified trypsin (Promega, Madison, WI, USA) in 30% ACN, 0.05 M ammonium bicarbonate, and 0.005 M DTT. This procedure for in-gel digestion was performed overnight at 30°C. The samples were lyophilized overnight with the use of Labconco Lyph-lock 1L Model 77400 (Labconco, Kansas, MO, USA) (7). Lyophilized samples were then dissolved in 0.1% formic acid (12).

LC-MS/MS. Peptide sequencing of identified protein spots was performed using an Agilent 1100 LC-MSD Trap XCT (Agilent Technologies, Palo Alto, CA, USA). Proteins were identified in an Agilent Spectrum Mill MS proteomics workbench against the Swiss-Prot protein database search engine (http://kr.expasy.org/sprot/) and MASCOT MS/MS Ions Search engine (http//www.matrixscience.com/search_form_select.html). Standards/parameters for induction of candidate proteins were set as follows: filter by protein score >10.0, and filter peptide by score >8.0. The Spectrum Mill workbench searched for MS/MS spectra, using an MS/MS ion search (13, 14).

Western blot analysis. Fifteen micrograms of whole-cell lysates were subjected to electrophoresis on 10% SDS polyacrylamide gels, and then transfered onto polyvinylidene fluoride (PVDF) membranes (immobilon; Millipore, Bedford, MA, USA). After blocking overnight at 4°C with Tris-buffered saline (TBS) containing 5% skimmed milk, the membranes were incubated with primary antibody against B-23 (mouse monoclonal antibody to nucleophosmin/NPM1; concentration 0.2 μg/ml; Sigma-Aldrich, St. Louis, MO, USA) at 4°C overnight, and then incubated with the secondary antibody conjugated with horseradish peroxidase (dilution 1:10,000; Jackson ImmunoResearch Laboratories Inc., West Grove, PA, USA) for 1 h at room temperature after washing three times with TBS containing Tween-20 and once with TBS. Membranes were then treated with a chemilluminescent reagent (ImmunoStar Long Detection; Wako, Osaka, Japan) and proteins were detected by using Image Reader LAS-1000 Pro (Fujifilm Corporation, Tokyo, Japan). Mouse monoclonal antibody against α-tubulin (dilution 1:200; Calbiochem, San Diego, CA, USA) was used for normalization of the proteins from western blot analysis.

Two-dimensional western blot analysis. Eighty micrograms of samples were separated on 2-DE gels and then transfer onto PVDF membranes at 90 mA for 78 min. The membranes were blocked overnight at 4°C with TBS containing 5% milk. Membranes were incubated with the primary antibody to NPM at 4°C overnight and then incubated with the secondary antibody conjugated with horseradish peroxidase for 1 h at room temperature. After washing three times with TBS containing Tween-20 and once with TBS, membranes were then treated with a chemilluminescent reagent and imaged using Image Reader LAS-1000 Pro.

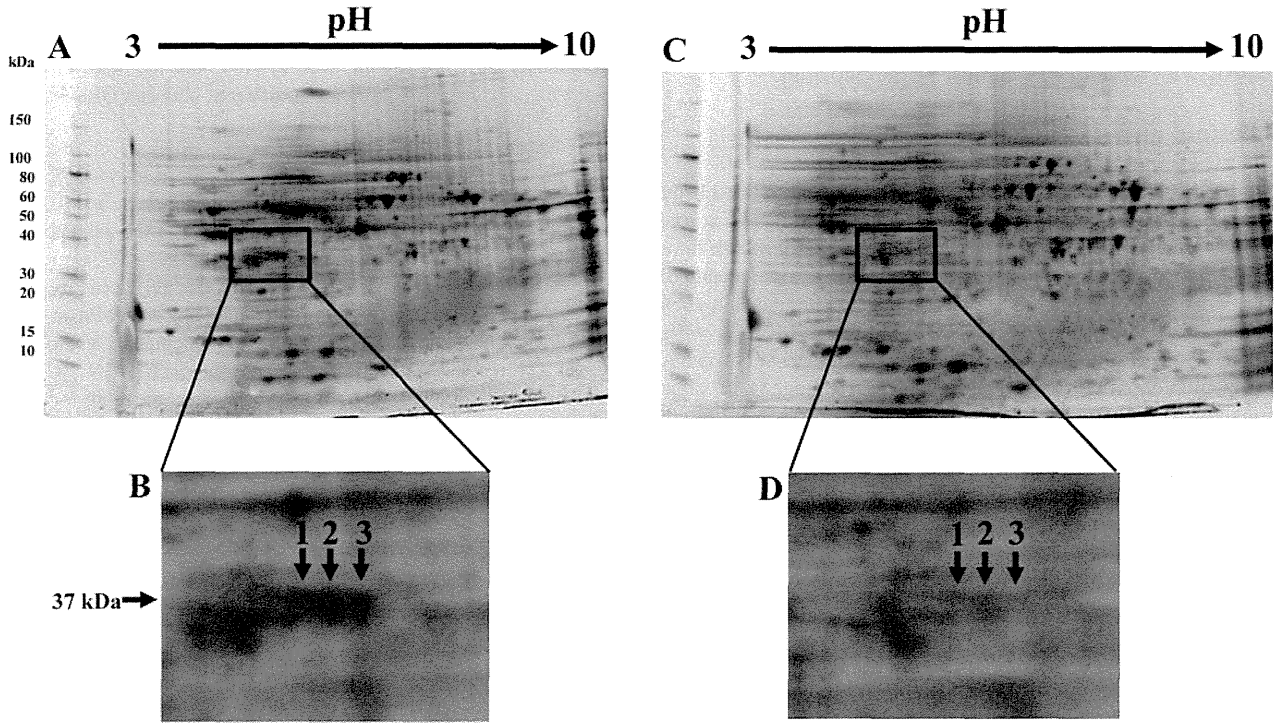

Figure 1. *Comparison of spots between QR-32 (A, B) and QRsP-11 (C, D) cells. In the square, arrows indicate three protein spots (numbered 1-3). These three spots were found to be weaker on 2-DE gels of QRsP-11 (D), compared to QR-32 (B).*

Table I. *Identification of the protein spots of down-regulated expression in QR-32 and QRsP-11 cells.*

Spot	Distinct peptides	MS/MS search score	Coverage (%)	Mass (Da)/pI	Accession no.*	Protein
1	8	106.10	28	32560.2/4.62	Q61937	Nucleophosmin
2	7	107.89	35	32560.2/4.62	Q61937	Nucleophosmin
3	4	60.09	23	32560.2/4.62	Q61937	Nucleophosmin

*Accession no. for SwissProt data base.

Results

Detection of protein spots on 2-DE gels. Many protein spots were visualized on the 2-DE gels. Among these, three protein spots (numbered 1-3) were found to be significantly weaker on 2-DE gels of QRsP-11 cells compared to QR-32 cells (Figure 1).

Identification of proteins by LC-MS/MS. Each spot provided a good spectrum of amino acids upon LC-MS/MS analysis, and was identified as NPM. MS and MS/MS spectra of trypsin-digested spots are shown in Figure 2 and Table I.

Western blot analysis. Regressive murine fibrosarcoma cell clone QR-32 exhibited a strong band of NPM, but its expression was very faint in progressive malignant cell clone QRsP-11 (Figure 3).

Two-dimensional western blot analysis of nucleophosmin isoforms. Three pairs of QR-32 and QRsP-11 were analyzed by 2-D western blotting analysis. Using a specific antibody against nucleophosmin, the spots were confirmed as being three NPM isoforms (Figure 4). The different isoforms were found to be significantly down-regulated in QRsP-11 cells compared to QR-32 cells.

Discussion

Nucleophosmin (also known as B23, NO38, or numatrin) is frequently conserved in vertebrates and widely distributed

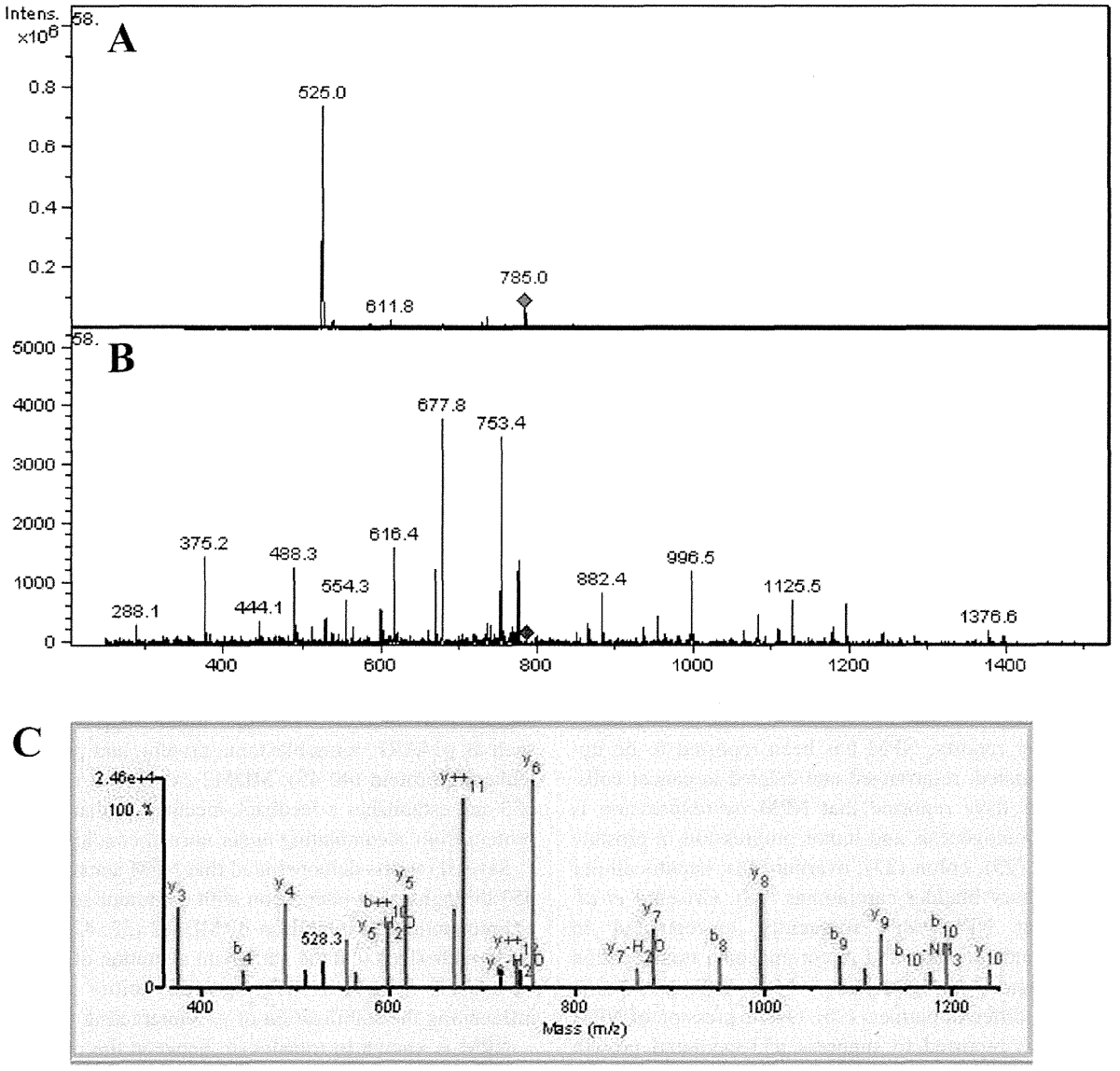

Figure 2. *Mass spectrometry (MS) and MS/MS spectra of trypsin-digested spot 1, shown in Figure 1. A: MS spectra of trypsin-digested spots; nucleophosmin precursor ion m/z is 785.0. B and C: MS/MS spectrum of a precursor ion with m/z 785.0 marked by a diamond in (A). The MS/MS spectrum identifies the partial tryptic peptide [K]VDNDENEHQLSLR[T] from nucleophosmin, processed with a spectrum Mill workbench.*

among different species, with a molecular weight of 35 to 40 kDa. In the human and rat, NPM exists at least with two isoforms, NPM1 and NPM1.2 (B23.1 and B23.2, respectively), which are generated from a single gene *via* alternate splicing (15). However, in mice, only NPM1 exists.

NPM is a non-ribosomal nucleolar phosphoprotein, implicated in cancer, which shuttles continuously between the nucleus and the cytoplasm (16). NPM is a multifunctional protein that is indispensable for various cellular processes including centrosome duplication, ribosome biogenesis, cell-cycle progression, apoptosis, transformation and genomic stability (17-20). Importantly, NPM displays several interrelated nucleolar functions that contribute to cell growth. Therefore, many researchers have focused their attention on these NPM activities and numerous attempts have been made to elucidate its role in cancer cells. Although the role of NPM in oncogenesis has been an object of study for a long time, this is still controversial because its precise role is complex.

NPM protein levels are generally correlated with mitogen-induced cell proliferation, and NPM fusion proteins are found in several malignancies (21). NPM would be expected to be a

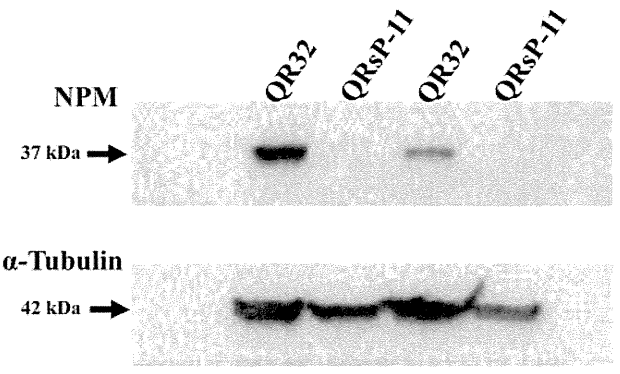

Figure 3. *Western blot analysis of nucleophosmin (NPM). Figure shows the band of NPM (37 kDa) and α-tubulin (42 kDa), as a loading control, in QR-32 and QRsP-11 cells.*

protein with proto-oncogenic activity, and in fact the NPM gene is a direct transcriptional target of the *c-MYC* proto-oncogene transcription factor (22). Moreover, NPM protein levels are elevated in dividing cells and cancer cells (23), but tend to decrease when cells differentiate and stop growing (18). Therefore, we focused our attention on NPM protein levels to possibly elucidate tumorigenesis in the present study.

From many reports, NPM has been reported to be up-regulated, mutated, re-arranged and deleted in cancer cells. Many studies have reported that NPM overexpression is related to carcinogenesis and tumor progression in prostate (24), gastric (25), colon (23), ovarian (26), hepatocellular (27) and urinary bladder carcinomas (28). Grisendi *et al.* reported that NPM was frequently up-regulated in carcinomas and was involved in chromosome translocation in hematological malignancies, where it forms fusion proteins with different partners (16). Overexpression of NPM has also been reported to suppress p53-mediated growth arrest and apoptosis, following exposure of cells to UV radiation or hypoxia (29, 30).

On the other hand, there are opposing reports for the studies described above. Li *et al.* reported that NPM protected cells from apoptotic cell death induced by diverse stresses through a mechanism involving inhibition of the p53 tumor-suppressor protein (31). They pointed-out that NPM might stabilize p53, a major regulator of apoptosis, or promote its degradation during nucleolar stress (31, 32). Our finding in this study supports their theory. There are conflicting reports on NPM levels (gain or loss of expression) and the effect of NPM on p53 activity.

The potent activity of p53 as inducer of cellular apoptosis and cell-cycle arrest demands tight control of its function. The major mode for provoking p53 action is DNA damage, which leads to the interaction between murine double minute 2 homolog (MDM2) and p53, increased p53 stability and activity (33). p53 activity is also induced by cellular oncogenes, such as *RAS* and *MYC* (34), and viral proteins such as viral cyclin (K cyclin) expressed by Kaposi's sarcoma-associated herpesvirus (35). *RAS* and *MYC* increase the levels of alternative reading frame (ARF), which binds MDM2 and translocates it to the nucleoli, relieving the negative regulation of p53 by MDM2 (36-38).

The stress response pathway that correlates with p53, p14 alternate reading frame (ARF) and MDM2 plays a central role in mediating cellular responses to oncogene activation, and genomic instability, and induces various forms of DNA damage. Recent studies pointed out that invalidation of the pathway results in many kinds of cancer, and may be crucial for tumor progression. One of the triggers of cell-cycle arrest and apoptosis induced by DNA damage is p53. It works as a transcription factor that serves as a point of convergence for various stress signals, such as DNA damage, oncogene activation and hypoxia-induced factor, all of which are common features of cancer cells. Activation of the p53 pathway centers on regulation of p53 protein stability and function (38). MDM2 is a p53 antagonist consisting of a nucleoplasmic and nucleolar really interesting new gene (RING)-finger protein that targets p53 degradation and inhibits p53 transcriptional activity through the proteasome (39). MDM2 also interacts with other tumor suppressor proteins, such as p14ARF, retinoblastoma protein, and promyelocytic leukemia protein (40-45). MDM2 expression is induced by p53 and establishes a feedback mechanism that prevents the protein from accumulating under normal conditions (46).

Several reports demonstrated that NPM actually stabilized p53 through direct interaction with the tumor suppressor and indirect action by inhibition of MDM2 (32, 47). Therefore, we hypothesized that the malignant alteration of tumor might be closely related to the specific ability of NPM in influencing the stabilization of p53 interacting with MDM2.

NPM is known to translocate between the nucleolus and nucleoplasm in response to cytotoxic drugs and genotoxic stress, such as inhibition of RNA polymerase I, DNA intercalating agents, and UV damage (48-50). NPM and MDM2 interact or co-localize increasingly, consequently to divergent cellular stresses, such as UV damage, proteasome inhibition, and expression of apoptosis-inducing viral proteins. Colombo *et al.* reported that high levels of ectopic NPM were seen to activate p53 and trigger p53-mediated growth arrest and cellular senescence in normal mouse embryo fibroblasts (MEFs), while promoting a slight stimulation of growth in *p53*-null MEFs (47). They pointed out that the effect of NPM in suppressing the early stages of tumorigenesis may be related to its role in maintaining genome stability and ensuring DNA integrity (47). Kurki *et al.* reported that p53 stabilization was augmented by rapid UVC-induced nucleoplasmic translocation of NPM and an increase in nucleoplasmic p53–NPM and MDM2–NPM

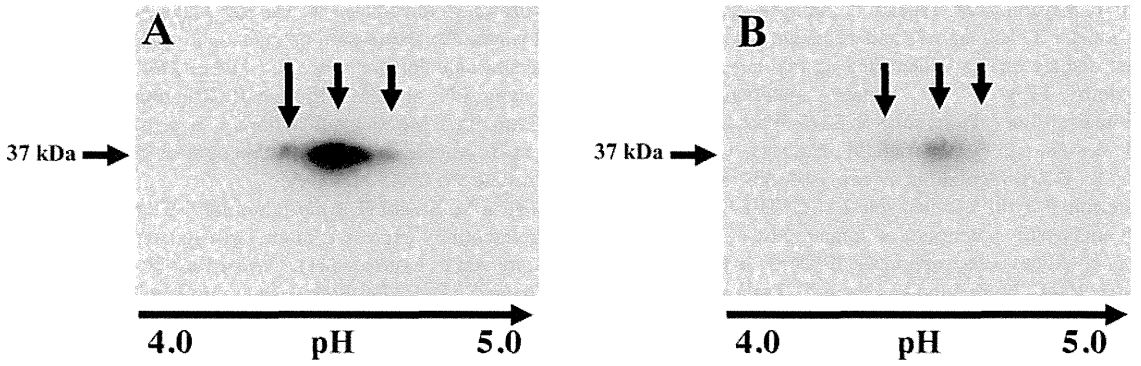

Figure 4. *Two-dimensional western blot analysis of nucleophosmin. Three spots of nucleophosmin can be seen in samples from QR-32 (A) and QRsP-11 (B) cells.*

complexes (32). They pointed-out that the dynamic re-organization of the complexes allows for early p53 stabilization and possibly assists in its modifications, such as sumoylation, commencing the subsequent stabilization effects. High levels of p53 competed for the interaction of NPM and MDM2 and depletion of NPM increased p53–MDM2 complex formation (32).

NPM can bind to p53 and regulate its stability and activity (47). Moreover, Kurki *et al.* reported that NPM tended to form complexes with MDM2 and may be unable to bind to and dissociate pre-formed p53–MDM2 complexes (32). They also indicated that the interaction of NPM with MDM2 was independent of p53 and is reduced *in vitro* by high levels of p53 (32). This suggests competition between p53 and MDM2 for binding sites on NPM.

The multiple interactions of NPM with cellular proteins suggest that it can act as a platform for protein interactions, affect their stabilization, or allow protein modifications to take place. Therefore, NPM could stabilize the complex formation between p53, MDM2, and other proteins needed for post-translational modifications in response to cellular stimulation. NPM might affect p53 stabilization through inhibition of its negative regulator, MDM2. Therefore, the depletion of NPM might cause the regressive tumor cells QR-32 to acquire progressive malignancy.

In this study, we performed 2-DE and MS to identify intracellular proteins expressed differentially in QR-32 and QRsP-11 cells, and we identified the intracellular protein NPM, whose expression differed between these two clones. The expression of NPM was down-regulated in the progressive tumor cells compared to the regressive tumor cells. It is possible that the tumor cells may acquire the malignant phenotypes in the course of progression *via* the dual function in regulation of p53 activity: by inhibiting p53 degradation through NPM interactions with MDM2, and by assembling complexes that are needed for p53 modifications, augmenting its activation and stabilization. Reduction of NPM might cause the stabilization of p53 and result in tumor progression.

Acknowledgements

We thank Dr. Byron Baron for proofreading the manuscript and discussions on this study. This study was supported in part by a Grant-in-Aid from the Japanese Ministry of Education, Science and Culture.

References

1 Okada F, Hosokawa M, Hamada JI, Hasegawa J, Kato M, Mizutani M, Ren J, Takeichi N and Kobayashi H: Malignant progression of a mouse fibrosarcoma by host cells reactive to a foreign body (gelatin sponge). Br J Cancer *66*: 635-639, 1992.

2 Ishikawa M, Hosokawa M, Oh-hara N, Niho Y and Kobayashi H: Marked granulocytosis in C57BL/6 mice bearing a transplanted BMT-11 fibrosarcoma. J Natl Cancer Inst *78*: 567-571, 1987.

3 Hayashi E, Kuramitsu Y, Okada F, Fujimoto M, Zhang X, Kobayashi M, Iizuka N, Ueyama Y and Nakamura K: Proteomic profiling for cancer progression: Differential display analysis for the expression of intracellular proteins between regressive and progressive cancer cell lines. Proteomics *5*: 1024-1032, 2005.

4 Kuramitsu Y, Hayashi E, Okada F, Tanaka T, Zhang X, Ueyama Y and Nakamura K: Proteomic analysis for nuclear proteins related to tumour malignant progression: A comparative proteomic study between malignant progressive cells and regressive cells. Anticancer Res *30*: 2093-2099, 2010.

5 Kuramitsu Y, Hayashi E, Okada F, Zhang X, Ueyama Y and Nakamura K: Two-dimensional gel electrophoresis using immobilized pH gradient strips and Flamingo™ Fluorescent Gel Stain identified non-nuclear proteins possibly relates to tumor malignant progression. Anticancer Res *31*: 1259-1263, 2011.

6 Habelhah H, Okada F, Kobayashi M, Nakai K, Choi S, Hamada J, Moriuchi T, Kaya M, Yoshida K, Fujinaga K and Hosokawa M: Increased E1AF expression in mouse fibrosarcoma promotes metastasis through induction of MT1-MMP expression. Oncogene *18*: 1771-1776, 1999.

7 Kuramitsu Y, Miyamoto H, Tanaka T, Zhang X, Fujimoto M, Ueda K, Tanaka T, Hamano K and Nakamura K: Proteomic differential display analysis identified up-regulated astrocytic phsphoprotein PEA-15 in human malignant pleural mesothelioma cell lines. Proteomics *9*: 5078-5089, 2009.

8 Tanaka T, Kuramitsu Y, Fujimoto M, Naito S, Oka M and Nakamura K: Down-regulation of two isoforms of ubiquitin carboxyl-terminal hydrolase isozyme L1 (UCH-L1) correlates with high metastatic potentials of human SN12C renal cell carcinoma cell clones. Electrophoresis *29*: 2651-2659, 2008.

9 Kuramitsu Y, Baron B, Yoshino S, Zhang X, Tanaka T, Yashiro M, Hirakawa K, Oka M and Nakamura K: Proteomic differential display analysis shows up-regulation of 14-3-3 protein sigma in human scirrhous-type gastric carcinoma cells. Anticancer Res *30*: 4459-4465, 2010.

10 Kuramitsu Y, Taba K, Ryozawa S, Yoshida K, Tanaka T, Zhang X, Maehara S, Maehara Y, Sakaida I and Nakamura K: Identification of up- and down-regulated proteins in gemcitabine-resistant pancreatic cancer cells using two-dimensional gel electrophoresis and mass spectrometry. Anticancer Res *30*: 3367-3372, 2010.

11 Kuramitsu Y, Hayashi E, Okada F, Zhang X, Tanaka T, Ueyama Y and Nakamura K: Staining with highly sensitive Coomassie brilliant blue SeePico™ stain after Flamingo™ fluorescent gel stain is useful for cancer proteomic analysis by means of two-dimensional gel electrophoresis. Anticancer Res *30*: 4001-4005, 2010.

12 Yuan X, Kuramitsu Y, Furumoto H, Zhang X, Hayashi E, Fujimoto M and Nakamura K: Nuclear protein profiling of Jurkat cells during heat stress-induced apoptosis by two-dimensional gel electrophoresis and tandem mass spectrometry. Electrophoresis *28*: 2018-2026, 2007.

13 Takashima M, Kuramitsu Y, Yokoyama Y, Iizuka N, Fujimoto M, Nishisaka T, Okita K, Oka M and Nakamura K: Overexpression of alpha enolase in hepatitis C virus-related hepatocellular carcinoma: Association with tumor progression as determined by proteomic analysis. Proteomics *5*: 1686-1692, 2005.

14 Takashima M, Kuramitsu Y, Yokoyama Y, Iizuka N, Harada T, Fujimoto M, Sakaida I, Okita K, Oka M and Nakamura K: Proteomic analysis of autoantibodies in patients with hepatocellular carcinoma. Proteomics *6*: 3894-3900, 2006.

15 Chang JH and Olson MO: Structure of the gene for rat nucleolar protein B23. J Biol Chem *265*: 18227-18233, 1990.

16 Grisendi S, Mecucci C, Falini B and Pandolfi PP: Nucleophosmin and cancer. Nat Rev Cancer *6*: 493-505, 2006.

17 Okuwaki M: The structure and functions of NPM1/nucleophosmin/B23, a multifunctional nucleolar acidic protein. J Biochem *143*: 441-448, 2008.

18 Hsu CY and Yung BY: Down-regulation of nucleophosmin/B23 during retinoic acid-induced differentiation of human promyelocytic leukemia HL-60 cells. Oncogene *16*: 915-923, 1998.

19 Okuda M: The role of nucleophosmin in centrosome duplication. Oncogene *21*: 6170-6174, 2002.

20 Lim MJ and Wang XW: Nucleophosmin and human cancer. Cancer Detect Prev 30: 481-490, 2006.

21 Grisendi S, Bernardi R, Rossi M, Cheng K, Khandker L, Manova K and Pandolfi PP: Role of nucleophosmin in embryonic development and tumorigenesis. Nature *437*: 147-153, 2005.

22 Zeller KI, Haggerty TJ, Barrett JF, Guo Q, Wonsey DR and Dang CV: Characterization of nucleophosmin (B23) as a myc target by scanning chromatin immunoprecipitation. J Biol Chem *276*: 48285-48291, 2001.

23 Nozawa Y, Van Belzen N, Van der Made AC, Dinjens WN and Bosman FT: Expression of nucleophosmin/B23 in normal and neoplastic colorectal mucosa. J Pathol *178*: 48-52, 1996.

24 Subong EN, Shue MJ, Epstein JI, Briggman JV, Chan PK and Partin AW: Monoclonal antibody to prostate cancer nuclear matrix protein (PRO: 4-216) recognizes nucleophosmin/B23. Prostate *39*: 298-304, 1999.

25 Tanaka M, Sasaki H, Kino I, Sugimura T and Terada M: Genes preferentially expressed in embryo stomach are predominantly expressed in gastric cancer. Cancer Res *52*: 3372-3377, 1992.

26 Zhang Y: The ARF-B23 connection: Implications for growth control and cancer treatment. Cell Cycle *3*: 259-262, 2004.

27 Liu X, Liu D, Qian D, Dai J, An Y, Jiang S, Stanley B, Yang J, Wang B, Liu X and Liu DX: Nucleophosmin (NPM1/B23) interacts with activating transcription factor 5 (ATF5) protein and promotes proteasome- and caspase-dependent ATF5 degradation in hepatocellular carcinoma cells. J Biol Chem *287*: 19599-19609, 2012.

28 Tsui KH, Cheng AJ, Chang PL, Pan TL and Yung BY: Association of nucleophosmin/B23 mRNA expression with clinical outcome in patients with bladder carcinoma. Urology *64*: 839-844, 2004.

29 Wu MH, Chang JH and Yung BY: Resistance to UV-induced cell-killing in nucleophosmin/NPM overexpressed NIH 3T3 fibroblasts: Enhancement of DNA repair and up-regulation of PCNA in association with nucleophosmin/B23 overexpression. Carcinogenesis *23*: 93-100, 2002.

30 Li J, Zhang X, Sejas DP, Bagby GC and Pang Q: Hypoxiainduced nucleophosmin protects cell death through inhibition of p53. J Biol Chem *279*: 41275-41279, 2004.

31 Li J, Zhang X, Sejas DP and Pang Q: Negative regulation of p53 by nucleophosmin antagonizes stress-induced apoptosis in human normal and malignant hematopoietic cells. Leukoc Res *29*: 1415-1423, 2005.

32 Kurki S, Peltonen K, Latonen L, Kiviharju TM, Ojala PM, Meek D and Laiho M: Nucleolar protein NPM interacts with HDM2 and protects tumor suppressor protein p53 from HDM2-mediated degradation. Cancer Cell *5*: 465-475, 2004.

33 Vousden KH and Lu X: Live or let die: The cell's response to p53. Nat Rev Cancer *2*: 594-604, 2002.

34 Sherr CJ: The INK4a/ARF network in tumour suppression. Nat Rev Mol Cell Biol *2*: 731-737, 2001.

35 Verschuren EW, Klefstrom J, Evan GI and Jones N: The oncogenic potential of Kaposi's sarcoma-associated herpesvirus cyclin is exposed by p53 loss *in vitro* and *in vivo*. Cancer Cell *2*: 229-241, 2002.

36 Weber JD, Taylor LJ, Roussel M, Sherr CJ and Bar-Sagi D: Nucleolar Arf sequesters Mdm2 and activates p53. Nat Cell Biol *1*: 20-26, 1999.

37 Weber JD, Kuo ML, Bothner B, DiGiammarino EL, Kriwacki RW, Roussel MF and Sherr CJ: Cooperative signals governing ARF–MDM2 interaction and nucleolar localization of the complex. Mol Cell Biol *20*: 2517-2528, 2000.

38 Lohrum, MA, Ashcroft M, Kubbutat MH and Vousden KH: Contribution of two independent MDM2-binding domains in p14(ARF) to p53 stabilization. Curr Biol *10*: 539-542, 2000.

39 Wadgaonkar R and Collins T: Murine double minute (MDM2) blocks p53-coactivator interaction, a new mechanism for inhibition of p53-dependent gene expression. J Biol Chem *274*: 13760-13767, 1999.

40 Barak Y and Oren M: Enhanced binding of a 95 kDa protein to p53 in cells undergoing p53-mediated growth arrest. EMBO J *11*: 2115-2121, 1992.
41 Momand J, Zambetti GP, Olson DC, George D and Levine AJ: The mdm-2 oncogene product forms a complex with the p53 protein and inhibits p53-mediated transactivation. Cell *69*: 1237-1245, 1992.
42 Haines DS, Landers JE, Engle LJ and George DL: Physical and functional interaction between wild-type p53 and mdm2 proteins. Mol Cell Biol *14*: 1171-1178, 1994.
43 Kamijo T, Weber JD, Zambetti G, Zindy F, Roussel MF and Sherr CJ: Functional and physical interactions of the ARF tumor suppressor with p53 and MDM2. Proc Natl Acad Sci USA *95*: 8292-8297, 1998.
44 Wei X, Yu ZK, Ramalingam A, Grossman SR, Yu JH, Bloch DB and Maki CG: Physical and functional interactions between PML and MDM2. J Biol Chem *278*: 29288-29297, 2003.
45 Kurki S, Latonen L and Laiho M: Cellular stress and DNA damage invoke temporally distinct MDM2, p53 and PML complexes and damage-specific nuclear relocalization. J Cell Sci *116*: 3917-3925, 2003.
46 Wu X, Bayle JH, Olson D and Levine AJ: The p53–mdm2 autoregulatory feedback loop. Genes Dev *7*: 1126-1132, 1993.
47 Colombo E, Marine JC, Danovi D, Falini B and Pelicci PG: Nucleophosmin regulates the stability and transcriptional activity of p53. Nat Cell Biol *4*: 529-533, 2002.
48 Wu MH and Yung BY: UV stimulation of nucleophosmin/B23 expression is an immediate-early gene response induced by damaged DNA. J Biol Chem *277*: 48234-48240, 2002.
49 Yang C, Maiguel DA and Carrier F: Identification of nucleolin and nucleophosmin as genotoxic stress-responsive RNA-binding proteins. Nucleic Acids Res *30*: 2251-2260, 2002.
50 Rubbi CP and Milner J: Disruption of the nucleolus mediates stabilization of p53 in response to DNA damage and other stresses. EMBO J *22*: 6068-6077, 2003.

Received November 1, 2012
Revised November 20, 2012
Accepted November 21, 2012

Proteomic differential display identifies upregulated vinculin as a possible biomarker of pancreatic cancer

YUFENG WANG[1], YASUHIRO KURAMITSU[1], TOMIO UENO[2], NOBUAKI SUZUKI[2], SHIGEFUMI YOSHINO[2], NORIO IIZUKA[2], XIULIAN ZHANG[1], JUNKO AKADA[1], MASAAKI OKA[2] and KAZUYUKI NAKAMURA[1]

Departments of [1]Biochemistry and Functional Proteomics and [2]Digestive Surgery of Applied Molecular Bioscience, Yamaguchi University Graduate School of Medicine, Ube, Japan

DOI: 10.3892/or_xxxxxxxx

Abstract. Pancreatic cancer (PC) is characterized by rapid tumor spread, and very few patients with PC survive for more than 5 years. It is imperative to discover additional diagnostic biomarkers or specific therapeutic targets in order to improve the treatment of patients with PC. In search for useful biomarkers, we analyzed ten pairs of non-cancerous and cancer tissues from patients with PC by two-dimensional gel electrophoresis (2-DE). Nineteen protein spots showed differential expression on 2-DE gels between the cancer and non-cancerous tissues. Six upregulated protein spots were identified by liquid chromatography-tandem mass spectrometry (LC-MS/MS) as calreticulin, glutathione synthetase, stathmin, vinculin, α-enolase and glyceraldehyde-3-phosphate dehydrogenase. Western blotting demonstrated that vinculin was predominantly expressed in the pancreatic cancer tissues compared with to non-cancerous tissues. Our findings indicate that vinculin may be a clinically useful biomarker of PC.

Introduction

Prognosis of patients with pancreatic cancer (PC) is poor because of belated diagnosis and lack of effective therapies. This disease is characterized by rapid tumor spread, and the median survival is less than 12 months with an overall 5-year survival rate of <5% (1). It is imminent therefore to find more effective biomarkers for the diagnosis of patients with pancreatic cancer and to clarify the biological characteristics of rapid aggressiveness of PC.

In recent years, proteomics has been widely applied to the identification of candidate biomarkers and therapeutic targets in various cancers (2-5). Two-dimensional gel electrophoresis (2-DE) and liquid chromatography-tandem mass spectrometry (LC-MS/MS) are the major proteomics techniques, which are utilized in analyzing proteins comprehensively.

The proteomics technology is an ideal option for finding biomarkers and therapeutic targets in cancer. By applying 2-DE and LC-MS/MS combined with western blotting, we found six differentially expressed proteins between pancreatic cancerous and non-cancerous tissues, and among them vinculin was identified as a potential biomarker for PC diagnosis or prognosis.

Materials and methods

Pancreatic tissues and sample preparation. Thirty pairs of non-cancerous and cancerous pancreatic tissues were obtained from 30 patients (Table I) who underwent resection of pancreas with diagnosis of pancreatic cancer at the Department of Surgery II, Yamaguchi University Hospital.

None of the patients received any preoperative therapy. Written informed consent was obtained from all patients before surgery. Tissues were obtained immediately after surgery and stored at -80°C until use. The study protocol was approved by the Institutional Review Board for Human Use of the Yamaguchi University School of Medicine. The tissues were homogenized in lysis buffer (1% NP-40, 1 mM sodium vanadate, 1 mM PMSF, 10 mM NaF, 10 mM EDTA, 50 mM Tris, 165 mM NaCl, 10 μg/ml leupeptin, and 10 μg/ml aprotinin) on ice (5). Suspensions were incubated for 2 h at 4°C, and the supernatants were stored at -80°C until they were used as samples. Ten pairs of samples were used for 2-DE, and twenty pairs for western blotting.

Two-dimensional gel electrophoresis (2-DE). As the first dimension, isoelectric focusing (IEF) was conducted in an IPGphor 3 IEF unit (GE Healthcare, Buckinghamshire, UK) on 11-cm and pH 3-10 linear gradient IPG strips (Bio-Rad, Hercules, CA, USA) at 50 μA/strip. Protein (80 μg) was used

Correspondence to: Dr Yasuhiro Kuramitsu, Department of Biochemistry and Functional Proteomics, Yamaguchi University Graduate School of Medicine, 1-1-1 Minami-Kogushi, Ube, Yamaguchi 755-8505, Japan
E-mail: climates@yamaguchi-u.ac.jp

Abbreviations: PC, pancreatic cancer; 2-DE, two-dimensional gel electrophoresis; LC-MS/MS, liquid chromatography-tandem mass spectrometry

Key words: two-dimensional gel electrophoresis, liquid chromatography-tandem mass spectrometry, pancreatic cancer, vinculin

Table I. Clinicopathological parameters of patients with pancreatic cancer.

No.	Age	Gender	TNM stage	Tumor grade
1[a]	79	Male	III	Moderately differentiated
2[a]	67	Male	III	Moderately differentiated
3[a]	54	Male	III	Moderately differentiated
4[a]	75	Male	IVb	Poorly differentiated
5[a]	71	Female	III	Well differentiated
6[a]	58	Male	IVb	Mucinous carcinoma
7[a]	70	Female	III	Moderately differentiated
8[a]	64	Male	III	Moderately differentiated
9[a]	61	Male	IVa	Moderately differentiated
10[a]	51	Female	II	Moderately differentiated
11	67	Male	IVa	Well differentiated
12	60	Female	III	Moderately differentiated
13	48	Female	IVa	Moderately differentiated
14	73	Male	IVa	Moderately differentiated
15	54	Male	IVa	Moderately differentiated
16	57	Male	IVb	Moderately differentiated
17	54	Male	III	Moderately differentiated
18	74	Female	IVa	Poorly differentiated
19	72	Male	III	Moderately differentiated
20	72	Male	IVa	Well differentiated
21	76	Female	IVa	Moderately differentiated
22	73	Female	III	Papillary carcinoma
23	53	Male	IVb	Well differentiated
24	69	Female	III	Moderately differentiated
25	79	Male	IVb	Mucinous carcinoma
26	34	Male	IVb	Acinor carcinoma
27	71	Female	III	Moderately differentiated
28	67	Female	IVa	Moderately differentiated
29	68	Male	III	Moderately differentiated
30	60	Male	IVb	Moderately differentiated

[a] indicates samples were used in 2-DE analysis.

for each 2-DE. Samples were mixed with 200 μl of rehydration buffer [8 M urea, 2% CHAPS, 0.01% bromophenol blue, 1.2% Destreak reagent (GE Healthcare)] and 0.5% IPG buffer, and loaded in the IPGphor strip holder. The strips were then focused by the following program: rehydration for 10 h (no voltage); 0-500 V for 4 h; 500-1,000 V for 1 h; 1,000-8,000 V for 4 h; 8,000 V for 20 min; and the final phase of 500 V from 20,000-30,000 Vh (6). After IEF, sodium dodecyl sulfate-polyacrylamide gel electrophoresis (SDS-PAGE) was performed on a precast polyacrylamide gel with a linear concentration gradient of 5-20% (Bio-Rad) (7). The IPG strips were first equilibrated in equilibration buffer 1 (6 M urea, 0.5 M Tris-HCl, pH 8.8, 30% glycerol, 2% SDS, 2% 2-ME) for 10 min, and further in equilibration buffer 2 (6 M urea, 0.5 M Tris-HCl, pH 8.8, 30% glycerol, 2% SDS, 2.5% iodoacetamide) for 10 min. The IPG strips were then transferred onto the gels, which were run at 200 V (8). Each sample was replicated three times to ensure protein pattern reproducibility.

Fluorescence staining. The SDS-PAGE gels were fixed with 40% ethanol and 10% acetic acid for 2.5 h. The gels were then treated with a fluorescent gel staining, Flamingo™ Fluorescent Gel Stain (Bio-Rad), for 18 h (9). The stained gels were washed with Milli-Q water 3 times, for 5 min each. These experimental procedures were carried out on a shaker.

Image analysis and spot picking. The gels were scanned by using the ProXpress 2-D Proteomic Imaging System (PerkinElmer, Waltham, MA, USA) and then analyzed by using the Progenesis SameSpots software (Nonlinear Dynamics, Newcastle, UK) following the user manual. After image analysis, the gels were stained with See Pico™ (Benebiosis Co., Ltd., Seoul, Korea) overnight (10). The selected protein spots that displayed different intensities were cut from the gels and subjected to mass spectrometry (MS) analysis.

In-gel digestion. The gel pieces were destained by rinsing three times in 60% methanol, 0.05 M ammonium bicarbonate,

Table II. Upregulated proteins in pancreatic cancerous tissues.

Spot	Accession no.[a]	pI[b]	Mr (Da)[b]	Spot intensity ratio	Frequency	Protein
1	P27797	4.29	48141.8	2.10	9/10	Calreticulin
2	P48637	5.67	52385.1	1.50	7/10	Glutathione synthetase
3	P16949	5.76	17302.6	1.50	5/10	Stathmin
4	P18206	5.50	123800.0	1.50	8/10	Vinculin
5	P06733	7.01	47169.2	1.60	9/10	α-enolase
6	P04406	8.57	6053.4	1.70	7/10	Glyceraldehyde 3-phosphate dehydrogenase

[a]Accession number derived from the protein database. [b]Theoretical pI and molecular weight (Da) from the protein database.

and 5 mM DTT for 15 min. The sample in the gel piece was reduced twice in 50% methanol, 0.05 M ammonium bicarbonate, and 5 mM DTT for 10 min. The gel pieces were dehydrated twice in 100% acetonitrile (ACN) for 30 min. Enzyme digestion was carried out with an in-gel digestion reagent containing 10 μg/ml sequencing-grade-modified trypsin (Promega Corporation, Madison, WI, USA) in 30% ACN, 0.05 M ammonium bicarbonate, and 5 mM DTT at 30°C for 16 h. The samples were lyophilized overnight with the use of Labconco Lyph-lock 1L Model 77400 (Labconco, Kansas, MO, USA).

LC-MS/MS analysis. The lyophilized samples were dissolved in 15 μl of 0.1% formic acid, and then analyzed by using the LC-MS/MS system. Peptide sequencing of identified protein spots was carried out by using LC-MS/MS with a Spectrum Mill MS Proteomics Workbench (Agilent Technologies, Palo Alto, CA, USA). Fifteen microliters of each sample was injected and placed into separated columns (Zorbax 300SB-C18, 75 μm, 150 mm, Agilent Technologies). The Agilent 1100 capillary pump was operated in the following conditions: solvent A, 0.1% formic acid; solvent B, ACN in 0.1% formic acid; column flow, 0.3 μl/min for primary flow, otherwise 300 μl/min; gradient, 0-5 min 2% B and 60 min 60% B; stop time: 60 min. Proteins were identified in the Agilent Spectrum Mill MS Proteomics Workbench against the Swiss-Prot protein database search engine (http://kr.expasy.org/sprot/) and MASCOT MS/MS Ions Search engine (http://www.matrixscience.com/search_form_select.html). Standards for induction of candidate proteins were set as follows: filter by protein score >10.0, and filter peptide by score >8 (percent scored peak intensity).

Western blotting. The samples were separated by electrophoresis with SDS-PAGE gels and then transferred onto PVDF membranes at 90 mA for 78 min. The membranes were blocked overnight with TBS containing 5% milk at 4°C (11). They were incubated with the primary antibody against vinculin (anti-vinculin mouse monoclonal antibody, Sigma, St. Louis, MO, USA; 1:10,000), α-enolase (anti-enolase goat polyclonal antibody, Santa Cruz Biotechnology, Inc., Santa Cruz, CA; 1:1,000) and actin (anti-actin goat polyclonal antibody, Santa Cruz Biotechnology, Inc.; 1:200). The membranes were incubated with the secondary antibody conjugated with horseradish peroxidase (1:10,000) for 1 h at room temperature after washing three times with TBS containing Tween-20 and once with TBS. The membranes were treated with the ImmunoStar® LD chemiluminescent reagent (Wako Pure Chemical Industries Ltd., Osaka, Japan), and protein spots were detected by using the Image Reader LAS-1000 Pro (Fujifilm Corporation, Tokyo, Japan).

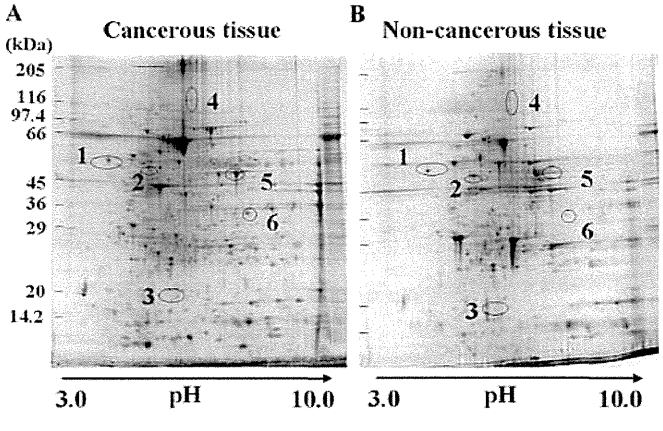

Figure 1. Two-dimensional gel electrophoresis images of pancreatic cancerous and non-cancerous tissues stained with Flamingo™ fluorescent gel stain. Proteins were separated on pH 3-10 linear, immobilized pH gradient strips followed by 5-20% SDS-PAGE. Six spots showed enhanced intensity on gels of cancerous tissues (A) compared to non-cancerous tissues (B). They were numbered as spots 1-6

Results

Detection of protein spots in pancreatic cancerous and non-cancerous tissues on 2-DE gels. 2-DE gels were treated with a fluorescent gel stain, and then differences in the spot intensities between the tissues from pancreatic cancer and non-cancerous were analyzed and quantified by using the Progenesis SameSpots software. The results are summarized in Table II. At least 260 protein spots were matched on each 2-DE gel. Six upregulated spots (spots 1-6) were displayed on 2-DE gel with cancerous tissues at >1.5-fold higher intensity (Fig. 1). The protein expression levels were elevated significantly ($P<0.05$) in cancerous tissues when compared to paired non-cancerous tissues (Fig. 2).

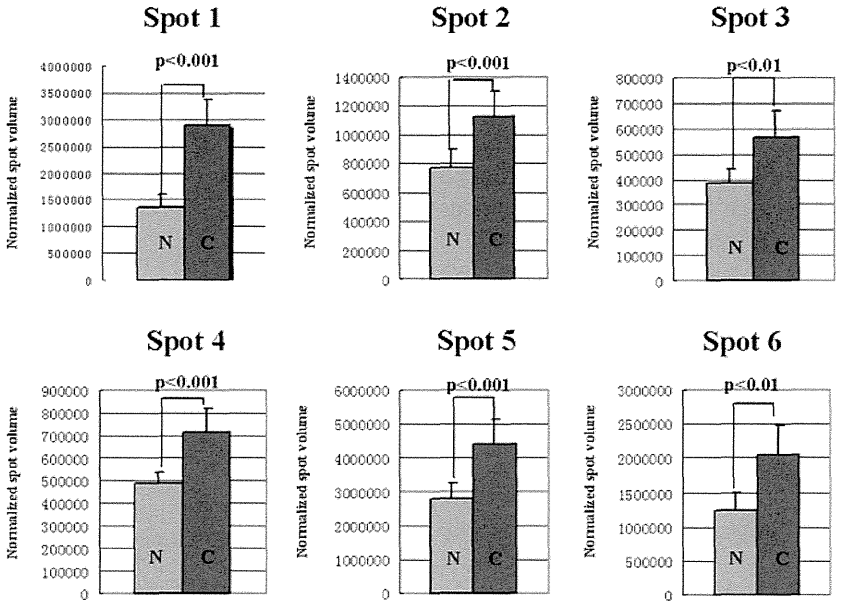

Figure 2. Enhanced protein expressions of carlreticulin (spot 1), glutathione synthetase (spot 2), stathmin (spot 3), vinculin (spot 4), α-enolase (spot 5) and glyceraldehyde-3-phosphate dehydrogenase (spot 6) in pancreatic cancerous tissues. The graphs show the normalized intensity of each spot in cancerous (C) compared to non-cancerous (N) tissues (n=30, P<0.05). Spot numbers are same as in Fig. 1.

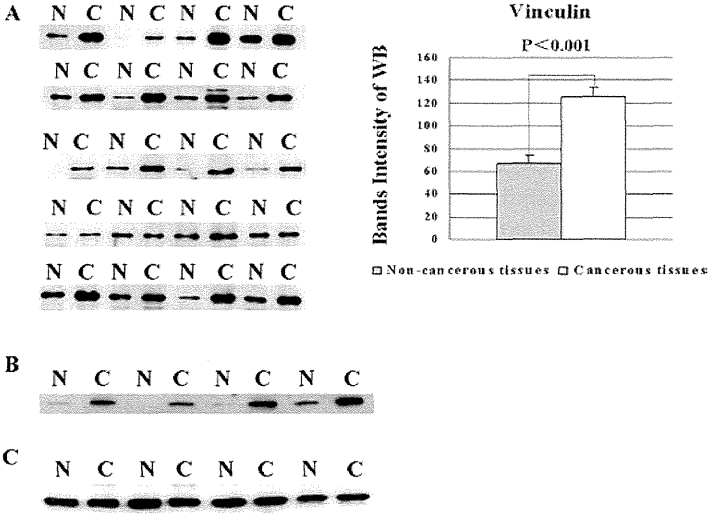

Figure 3. Western-blot analyses of vinculin and α-enolase in pancreatic cancerous and non-cancerous tissues. (A) Tissues from 20 patients with pancreatic cancerous and paired non-cancerous tissues were used for western blotting with anti-vinculin antibody. The expression of vinculin was increased in pancreatic cancerous tissues (80%). Intensities of the bands were compared between cancerous and non-cancerous tissues by Student's t-test (n=20, P<0.001). The relative standard errors (SE) of cancerous and non-cancerous tissue samples were 8.438 and 7.695, respectively. Expressions of α-enolase (B) and actin (C) were confirmed by western blotting respectively; the intensity of each band of α-enolase was stronger in cancerous tissues than in non-cancerous tissues. N, non-cancerous tissues; C, cancerous tissues.

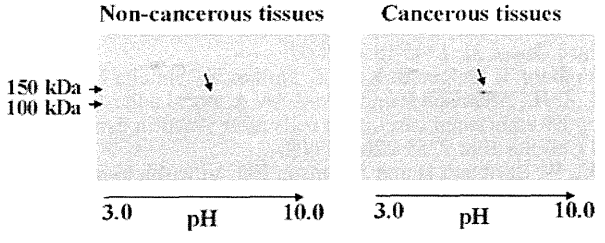

Figure 4. Two-dimensional (2-D) western blotting of vinculin in pancreatic cancerous tissues. Two-dimensional western blotting was performed on a pair of samples on pH 3-10 linear, which confirmed the locations of vinculin on PVDF membranes. The upregulated spot of vinculin was observed in cancerous tissue, compared to non-cancerous tissues.

Identification of proteins by LC-MS/MS. The samples were digested with trypsin and then analyzed by using LC-MS/MS system, which identified the six upregulated protein spots as calreticulin (spot 1), glutathione synthetase (spot 2), stathmin (spot 3), vinculin (spot 4), α-enolase (spot 5) and glyceraldehyde-3-phosphate dehydrogenase (spot 6). The spot numbers are the same as those in Fig. 1. MS/MS data of these proteins are summarized in Table II.

Western blot analysis of vinculin and α-enolase. There are still no reports regarding overexpression of vinculin in PC and its importance for cell adhesion and migration (12,13).